

Factorization for DIS, mostly in simple field theories

In this chapter, I treat the complications caused by renormalizability of the underlying field theory when one analyzes the asymptotics of processes like DIS. There are four inter-related issues:

- The leading regions include hard-scattering subgraphs that can be of arbitrarily high order in the coupling.
- There are logarithmic unsuppressed contributions from momenta that interpolate between the different regions for a graph.
- The definitions of the parton densities are modified to remove their UV divergences. This we do by renormalization.
- The parton densities acquire a scale argument μ , the dependence on which is governed by renormalization-group (RG) equations, the famous Dokshitzer-Gribov-Lipatov-Altarelli-Parisi (DGLAP) equations. In applications, we set μ of order Q , the large scale in the hard scattering.

I will give a derivation of factorization that in the absence of gauge fields is complete and satisfactory, and is also reasonably elementary. In QCD, the same factorization theorem is also valid for simple processes, like DIS, but its derivation needs enhancement, to be given in later chapters.

8.1 Factorization: overall view

To motivate the factorization idea, we still use the ideas about the space-time structure of DIS that motivated the parton model. As illustrated in the spatial diagram of Fig. 8.1, an electron undergoes a wide-angle hard scattering off a single parton in a high-energy target hadron. In the center-of-mass frame, the target is time-dilated and Lorentz contracted. Thus over the short time and distance scale $1/Q$ of the hard scattering, the struck parton's interactions with the rest of the target can be neglected; in the hard scattering, the incoming parton can be approximated as a free particle. A single struck parton dominates, because the other partons are separated from it by a hadronic scale of ~ 1 fm, large compared with $1/Q$.

Relative to the parton model, an important change in a renormalizable theory is that the dimensionlessness of the coupling allows multiple particles to be created in the hard

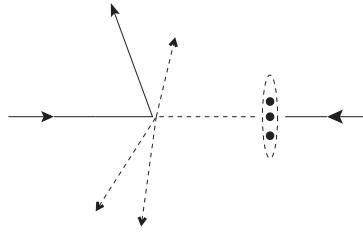


Fig. 8.1. Deeply inelastic scattering of an electron on a hadron. This is like Fig. 2.2, but with more partons exiting the short-distance hard scattering. The struck parton and the partons resulting from the hard scattering are indicated by dashed lines.

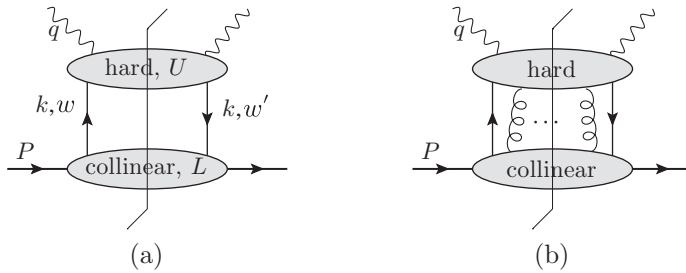


Fig. 8.2. Most general leading regions for DIS. The lines in the lower bubble are collinear to the target hadron, and the lines in the upper bubble have large transverse momentum, of order Q . (a) In a theory without gauge fields, exactly one line on each side of the final-state cut joins the two bubbles. The labels ω and ω' are for the flavor, color and spin of the intermediate parton lines. (b) In a theory with gauge fields, arbitrarily many extra gauge-field lines may join the bubbles. The solid lines may be quarks or transversely polarized gluons. In a gauge theory there may also be a soft subgraph at leading power.

scattering without a power-law suppression. This is manifested experimentally in events like that in Fig. 5.10. Naturally, an appropriate coupling for the short-distance scattering is $\alpha_s(Q)$, whose smallness in QCD allows the use of perturbation theory.

Our calculations in Sec. 6.11 showed another consequence of a dimensionless coupling, that the number density of partons only falls off in transverse momentum roughly as $1/k_T^2$. Therefore the number of partons, integrated over k_T , and naively interpreted, diverges. The picture of limited transverse momentum for the constituents, implicit in Fig. 8.1, therefore needs to be distorted.

The formalization of these ideas starts from the Libby-Sterman analysis in Ch. 5, which determines that the leading regions for DIS are those illustrated in Fig. 8.2.

8.1.1 Leading-power regions without gauge fields

In a model field theory without gauge fields, all the leading regions are of the form of Fig. 8.2(a). The lower bubble consists of lines whose momenta are collinear to the target. The upper bubble consists of lines with very different directions than the target or that are far off-shell. On each side of final-state cut, one line connects the collinear subgraph to the hard subgraph. This corresponds to the single struck parton in Fig. 8.1. Scattering off

multiple partons would correspond to extra lines connecting the upper and lower bubbles in Fig. 8.2(a), and is power-suppressed, by Libby and Sterman's power-counting.

While keeping the restriction to this single pair of connecting lines, the upper subgraph can be arbitrarily complicated. This gives the possibility of multijet production, as seen experimentally in Fig. 5.10. Associated with this is an essential complication, that a single graph for DIS can have multiple decompositions of the form of Fig. 8.2(a).

The upper bubble, the "hard subgraph", has on-shell final-state lines, but we will nevertheless treat it as if it is a short-distance object, with all internal lines off-shell by order Q^2 . The demonstration uses arguments given in Secs. 4.1.1, 4.4, and 5.3.3, where the short-distance property applies to a local average in the cross section (e.g., an average in x). Further details are found later in Secs. 11.2 and 12.7.

8.1.2 Leading-power regions with gauge fields

In a gauge theory, like QCD, leading regions can also have extra target-collinear gluons attaching to the hard scattering, as in Fig. 8.2(b). In the methodology where we treat the upper bubble as a pure hard scattering, this exhausts the leading regions; this applies, for example, to the uncut hadronic tensor and the structure functions averaged in x , as in Sec. 5.3.3. But it is also possible to consider the actual on-shell final states in the upper bubble; in that case there are final-state jet subgraphs, and a soft subgraph that connects any or all of the collinear subgraphs.

We now use the first methodology. The leading part of each extra gluon exchange involves the product of the minus component of the vertex at the upper end of the gluon line and a plus component at the lower end, schematically U^-L^+ . Thus the extra gluons can be eliminated by the use of the light-cone gauge, $A^+ = 0$: in light-cone gauge, the leading regions have the same form, Fig. 8.2(a), as in a non-gauge theory.

Therefore once we have proved factorization in a non-gauge theory, which is done in an elementary fashion in this chapter, we can copy the proof in light-cone-gauge QCD. To take it literally, one must be concerned about problems with the $1/k^+$ singularities in the light-cone-gauge gluon propagator, (7.30) and (7.31). These problems will become particularly apparent when we work with TMD distributions in Ch. 13. Nevertheless, divergences due to the $1/k^+$ singularities cancel in the treatment of DIS, although giving a full satisfactory proof is non-trivial.

For a fully satisfactory treatment, it will be better to return to Feynman gauge. We have already seen, in Sec. 7.7, that at the level of the parton model, the extra gluons can be extracted from the hard scattering to give the Wilson lines in gauge-invariant definitions of the parton densities. This is a result that generalizes, but I postpone a treatment to Ch. 11.

8.2 Elementary treatment of factorization

Before going to a strict derivation of factorization in non-gauge theories, it is useful to give an approximate proof. Its inspiration is a naive interpretation of the diagram Fig. 8.2(a) for the leading regions. This is that the momenta of lines can be unambiguously split into two classes, corresponding to the two subgraphs in the figure. Hard momenta, in the upper

subgraph U , have virtualities of order Q^2 . Collinear momenta, in the lower subgraph L , have orders of magnitude typical for target momenta, i.e., $(k^+, k^-, k_T) \sim (Q, m^2/Q, m)$, where m is a typical light hadron scale; their virtualities stay fixed when Q becomes large.

This supposition enables a simple proof to be given, and gives a mental picture linking the leading-region diagram Fig. 8.2(a) with the factorization formula. We will take the opportunity to introduce notation that will be useful more generally.

But a clear division between the regions of momenta does not exist; there are important contributions from intermediate momenta. We will overcome this problem by the use of a subtractive formalism, in Sec. 8.9.

8.2.1 Decomposition by regions

We now start from an assumption that there is a clear decomposition of momenta by regions. Then we can decompose each graph into a sum of terms of the form of Fig. 8.2(a), each term corresponding to a particular assignment of momentum types to subgraphs. Let F denote a structure function or the hadronic tensor. Then we have

$$\begin{aligned} F &= \sum_{\text{2PR graphs } \Gamma} \Gamma + \text{non-leading power} \\ &= \sum_{\text{2PR graphs } \Gamma} \sum_{\text{leading regions } R} U(R)L(R) + \text{non-leading power}, \end{aligned} \quad (8.1)$$

where the summation over Γ is restricted to those graphs that are two-particle reducible in the t channel and that therefore have at least one decomposition of the form of Fig. 8.2(a). A region R corresponds to assignments of momentum types to subgraphs, and is determined by the subgraphs: $U(R)$ for the upper bubble, restricted to hard momenta, and $L(R)$ for the lower bubble, restricted to collinear momenta. We define $L(R)$ to include the full propagators for the two lines that join the L and U subgraphs, since these lines carry collinear momenta.

The product $U(R)L(R)$ is defined as a convolution product, with an integral over the momentum k flowing between U and L , and with summations over the color, spin and flavor indices for the fields. So we write $U = U(k, \omega, \omega'; q)$ and $L = L(k, \omega, \omega'; P, S)$, where ω and ω' are composite indices for the flavor, color and spin of the fields, while P and S are the momentum and spin vector of the target state. Then

$$UL = \sum_{\omega, \omega'} \int \frac{d^{4-2\epsilon} k}{(2\pi)^{4-2\epsilon}} U(k, \omega, \omega'; q) L(k, \omega, \omega'; P, S). \quad (8.2)$$

A region is completely specified by its hard and target subgraphs, so we replace the sum over graphs and regions by independent sums over graphs for $U(R)$ and $L(R)$. So we write

$$F = UL + \text{non-leading power}, \quad (8.3)$$

where U and L , without a region specifier, are the sum over all possibilities for the hard and target-collinear subgraphs of Fig. 8.2(a), with the momenta being restricted to the appropriate regions.

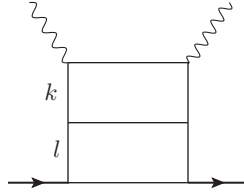


Fig. 8.3. Graph with three decompositions of the form of Fig. 8.2(a).

In (8.3) we have a *multiplicative* structure: the structure function is a product of a hard part and a collinear part. In contrast, at the level of individual graphs for the structure function, we have an *additive* structure: in the second line of (8.1) there is a sum over regions for a given graph. An illustration is given by Fig. 8.3. The possible regions are: where the top rung alone is hard, where the top two rungs are hard, and where all three rungs are hard.

Diagonality in flavor and color

In the convolution of U and L , there is a sum over indices ω and ω' , which we now simplify. For QCD, each index has 88 independent values: There are 6 flavors of quark, of antiquark, and a gluon. The quarks and antiquarks each have 3 colors, the gluons have 8, and each flavor-color combination has 2 spin values. We can separate the parts of the index ω as j, c and α , for flavor, color and spin. Here we refer to the QCD version even though in this chapter we will only present proofs in a non-gauge theory: the ideas are general.

In principle, there are separate sums over the indices ω and ω' for the two parton lines connecting U and L . I now show that the sums over flavor and color indices are diagonal in the cases of interest; i.e., the flavor and color parts of ω and ω' are equal.

We choose the flavor label to correspond to the different types of mass eigenstate for the partons (e.g., u, d , etc.). Normal targets (nucleons and pions) are flavor eigenstates, so the lower subgraph L is flavor-diagonal. An exception would be DIS on a K_L^0 or K_S^0 , which is not a likely experiment. Note that, for charged-current weak-interaction processes, the upper subgraph U can be flavor changing. Thus, in neutrino DIS, we can have the sequence of quark flavor transitions $d \mapsto u \mapsto s$. But diagonality of L implies that off-diagonal terms in U do not contribute.

As for color, all electroweak currents are color-singlet. Therefore U is diagonal in color, and all the diagonal color components of U are equal.

In contrast the spin-sum need not be diagonal. So we rewrite (8.2) as

$$F = \sum_{j,\alpha,\alpha'} \int \frac{d^{4-2\epsilon}k}{(2\pi)^{4-2\epsilon}} U(k, j, \alpha, \alpha'; q) \sum_c L(k, j, c, \alpha, \alpha'; P, S) + \text{non-leading power.} \tag{8.4}$$

Here we have left a single flavor label j on U and L , and a single color label c on L . The remaining sum, over α and α' , is for Dirac spin indices. The U part can be considered a color average, as will fit its later interpretation in terms of a parton-level cross section.

8.2.2 Parton approximator

To get the factorization theorem, we use exactly the same method we applied in Sec. 6.1 for the parton model. (a) In U we neglect the small components of momenta, k^- and \mathbf{k}_T , entering it from L , and we also neglect particle masses. (b) In the sum over Dirac indices, we project onto those parts that give the leading power. This operation, which we call the parton approximator, results in an error that is suppressed by one or two powers of Q .

We notate the result as

$$U \overleftarrow{T} |VL = C_{\text{region}} \otimes f_{\text{region}} \stackrel{\text{def}}{=} \sum_j \int \frac{d\xi}{\xi} C_{j, \text{region}}(x, \xi) f_{j, \text{region}}(\xi), \quad (8.5)$$

which is a factorized form for the cross section. Here we have defined a fractional momentum variable $\xi = k^+/P^+$. The tripartite symbol $\overleftarrow{T} |V$ denotes the parton approximator, for which we will give a precise definition below. The arrow in \overleftarrow{T} implies that the kinematic part of the approximation is applied to the object to its left, i.e., to U . The quantity V symbolizes the vertex for a parton density that is a factor in the approximator. We separate these symbols by a vertical bar, which will be a useful notation in treating renormalization of the parton densities. Although the above formula makes it appear that the parton approximator is a linear operator, certain features of the approximator, notably that it sets to zero the parton masses in U , take us beyond ordinary linear algebra. Even so, many of the rules of linear algebra still apply.

The parton approximator will give a factor that has a vertex for a parton density integrated with the L factor. Therefore on the right-hand side of (8.5), we have used a notation to express this. The resulting object has the standard definition of a parton density, except that the momenta inside L are restricted to be collinear. So f is equipped with a subscript “region”, to label this variation in the definition. A parton density is a function of just one kinematic argument ξ , so we represent the corresponding kind of convolution by the symbol \otimes , which is defined as on the rightmost part of the equation. The quantity C is the approximated U , but with a particular normalization. It goes by several names: coefficient function, short-distance partonic scattering, Wilson coefficient. To save extra notational complication, only the unpolarized terms are written explicitly.

Kinematic approximation

The first, kinematic, part of the approximator gives

$$F = \sum_{j, \alpha, \alpha'} \int_{x^-}^{1+x^-} \frac{d\xi}{\xi} U(\hat{k}, j, \alpha, \alpha'; q, m = 0) \\ \times \sum_c \int \frac{dk^- d^{2-2\epsilon} \mathbf{k}_T}{(2\pi)^{4-2\epsilon}} \xi P^+ L(k, j, c, \alpha, \alpha'; P, S) + \text{non-leading power.} \quad (8.6)$$

Here, we have changed variable from k^+ to ξ , and we have defined $\hat{k} = (\xi P^+, 0, \mathbf{0}_T)$, for the approximated parton momentum in U . The integral over k^- and \mathbf{k}_T is now confined to the L factor, as in a parton density, and we included with it a factor of ξP^+ for the sake of

boost invariance. The upper limit on ξ is imposed by the parton density, for positivity of the energy in its final state, $P^+ - \xi P^+ \geq 0$. The lower limit is set from positivity of the energy in the hard part of the graph, $q^+ + \xi P^+ \geq 0$. In general, the integrand can be a generalized function (distribution) with singularities at the endpoints. For example, there can be delta functions at $\xi = 1$ in L , and at $\xi = x$ in U (after approximation). The singularities are properly treated if we take the range of integration over ξ to extend beyond the kinematic limits, so I notate the limits as $x-$ and $1+$.

Approximator for scalar parton

When j denotes a scalar parton, there are no spin labels, so (8.4) gives the definition of $U \overleftarrow{T} |VL$ for a scalar quark:

$$(U \overleftarrow{T} |VL)_{\text{scalar } j} \stackrel{\text{def}}{=} \int_{x-}^{1+} \frac{d\xi}{\xi} U(q; \hat{k}, j; m = 0) \times \sum_c \int \frac{dk^- d^{2-2\epsilon} \mathbf{k}_T}{(2\pi)^{4-2\epsilon}} \xi P^+ L(k, j, c; P, S). \tag{8.7}$$

The second line, including the color sum and the factor ξP^+ , reproduces exactly the definition of the density of a scalar quark, (6.124). The first factor, the approximated U , has the normalization appropriate to DIS on an on-shell massless parton target, but with internal momenta restricted to being in the hard region. The integral joining the two factors is a convolution with measure $d\xi / \xi$, which we choose as its standard form.

Approximator for spin-1/2 parton

When j denotes a fermion quark, we have two formulations. One involves projection matrices \mathcal{P}_A and \mathcal{P}_B on each line, as in (6.13). The other reorganizes this, as in (6.19), into terms involving different kinds of spin-projected parton density. Thus we have

$$(U \overleftarrow{T} |VL)_{\text{Dirac } j} \stackrel{\text{def}}{=} \sum_{\alpha, \beta, \alpha', \beta'} \int dk^+ U(q; \hat{k}, j, \alpha, \alpha'; m = 0) \times (\mathcal{P}_A)_{\alpha\beta} (\mathcal{P}_B)_{\beta'\alpha'} \sum_c \int \frac{dk^- d^{2-2\epsilon} \mathbf{k}_T}{(2\pi)^{4-2\epsilon}} L(k, j, c, \beta, \beta'; P, S) = \int \frac{d\xi}{\xi} \text{Tr}_D \left[U(q; \hat{k}, j; m = 0) \frac{\hat{k}}{2} \right] \sum_c \int \frac{dk^- d^{2-2\epsilon} \mathbf{k}_T}{(2\pi)^{4-2\epsilon}} \text{Tr}_D \frac{\gamma^+}{2} L(k, j, c; P, S) + \text{terms with polarized parton densities.} \tag{8.8}$$

The factor $\hat{k}/2$ is exactly the external line factor for U that corresponds to a spin-averaged on-shell Dirac particle. See (6.19) and the preceding definitions (6.17) and (6.18) for the form of the polarized terms. They can be allowed for by replacing the factor $\hat{k}/2$ by the form (A.27) with polarization for the quark.

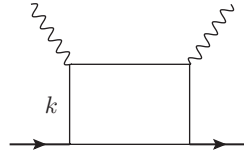


Fig. 8.4. One-loop graph for DIS in a model theory. The lines may represent any kind of field.

8.2.3 Factorization

We have now completed the definition of the parton approximator, and the result is a factorization of the form shown in (8.5).

8.2.4 Why the simple derivation does not work

The above derivation of the factorization theorem would be valid if one could use a fixed decomposition of momentum space into regions appropriate for U and L , at least up to power-suppressed terms. But in renormalizable theories, no clear separation of scales can be made. The issue is quite generic, so I illustrate it by examining a one-loop graph related to the calculations, in Sec. 6.11, of UV divergences in parton densities.

Consider a one-loop graph for DIS with an elementary-particle target, Fig. 8.4. We perform the k^\pm integrals by the mass-shell delta functions for the two final-state particles, to leave only an integral over k_T^2 . By the Libby-Sterman analysis, we obviously have leading-power contributions when k_T^2 is comparable to m^2 and when it is comparable to Q^2 ; these correspond, respectively, to regions where only the top rung is the hard subgraph, and where the whole graph is the hard subgraph.

But, as we now show, there is also a leading contribution from intermediate momenta, i.e., where $m \ll k_T \ll Q$. Since $k_T \ll Q$, we can apply the parton-model approximation to the top rung, and replace the calculation by the calculation of a parton density, as in Sec. 6.11. Then because, $m \ll k_T$, we can neglect m , thereby obtaining a logarithmic integral:

$$\text{constant} \times \int_{\sim m^2}^{\sim Q^2} \frac{dk_T^2}{k_T^2}. \quad (8.9)$$

That this is a logarithmic integral follows from the fact that the couplings are dimensionless. The whole graph has the same dimension as a lowest-order graph. Hence the momentum integral is dimensionless. Corrections to this formula are suppressed by powers of k_T/Q and of m/k_T .

Each range of a factor of 2 (say) in k_T^2 gives the same contribution. This contribution is also comparable in size to that from the hard range, $k_T \sim Q$, and from the collinear range, $k_T \sim m$. There is therefore no power-suppression (in m/Q) of the intermediate region. Indeed the intermediate region is slightly enhanced, i.e., logarithmically, by a factor $\ln(Q/m)$.

The elementary proof in Secs. 8.2.1–8.2.3 relied on a strict separation of scales: some momenta have $k_T \sim m$ and some have high virtuality, $O(Q^2)$, with unimportant contributions from intermediate momenta. When this is valid, errors of order m/Q result from neglecting k_T relative to Q . But the logarithmic contribution from the intermediate region violates the initial assumption.

One could try rescuing the argument by using an intermediate scale μ to separate collinear and hard momenta. In a one-loop graph this would result in errors of order μ/Q and of order m/μ : the first is from neglecting collinear transverse momenta relative to Q , and the second error is from neglecting masses with respect to hard momenta. The minimum error is of order $\sqrt{m/Q}$, obtained when $\mu \sim \sqrt{mQ}$. This is very non-optimal compared with the m/Q error (modified by logarithms) that is obtained from a better derivation of factorization.

Moreover in higher-order graphs, like Fig. 8.3, the errors from using a simple cutoff to separate the regions are actually unsuppressed. To see this consider a configuration in which the transverse momentum l_T in the lower loop of Fig. 8.3 is slightly below the cutoff, while k_T in the upper loop is slightly above the cutoff. Then l is target-collinear while k is hard. The elementary derivation tells us to neglect k_T with respect to l_T , producing a 100% error.

So we need a more powerful method, which we will come to in due course.

8.3 Renormalization of parton densities

We saw in calculations, Sec. 6.11, that parton densities have UV divergences at or above the space-time dimension $n = 4$ where the theory has a dimensionless coupling. This is one symptom that the parton model is not strictly correct. The Feynman graphs and momentum region that give the parton model still exist in such theories, but there are additional contributions.

In such a situation parton densities continue to be useful, but we have to adjust the definitions to make the parton densities finite. Motivated by what happens with the operator product expansion (OPE), reviewed in Collins (1984), we now construct such a definition by applying conventional UV renormalization. This gives renormalized parton densities as theoretical constructs, which can be studied in and of themselves, without regard to applications. Of course, it is the applications that provide *post hoc* motivation for studying parton densities.

8.3.1 Cutoff or renormalization?

An alternative to renormalization is to impose a cutoff in transverse momentum, e.g., to modify (6.75) to

$$f_{j/h}(\xi) \stackrel{\text{def}}{=} \int_{k_T < \mu} d^2 \mathbf{k}_T f_{j/h}(\xi, \mathbf{k}_T). \quad (8.10)$$

This definition has been particularly advocated by Brodsky and his collaborators (e.g., Lepage and Brodsky, 1980; Brodsky *et al.*, 2001) and clearly has certain advantages. Both

kinds of definition, by a cutoff and by renormalization, are legitimate, and there is a choice between them influenced by practicalities and by actual practice, not by absolute necessity. Recall the calculation in Sec. 3.4, where we showed that renormalization with a scale μ is similar to a cutoff at approximately the same scale. Thus the two kinds of definition of finite parton densities have similar properties and intuitive meanings. But one must not take the equivalence between renormalization and a cutoff as a strict mathematical property.

Serious work beyond leading order, or beyond leading-logarithm approximation, requires us to take the definitions rather literally. Here certain disadvantages of the cutoff method appear that lead us to use the renormalization method. One is simply that although the cutoff method lends itself very nicely to getting an overall view, detailed calculations can be harder. A second rather severe disadvantage is that the definition with a cutoff relies on the definition of the unintegrated or TMD density. Now, in a gauge theory, the basic definition of the unintegrated parton density entails the use of light-front gauge $A^+ = 0$. But this results in further divergences even before the k_T integral, and therefore requires even more complicated redefinitions (Ch. 13). This problem is often hidden in elementary discussions, but comes to the forefront once higher-order corrections are considered correctly and is a continuing topic of research and debate.

8.3.2 Statement of renormalization of parton densities

In the theory of renormalization (e.g., Collins, 1984) there are two ways of viewing the renormalization of composite operators. One is the multiplicative view, where renormalized operators are factors times the bare operators. The other view is the counterterm view, where for each Feynman graph a series of counterterms is subtracted to remove the divergences. It is very useful to switch between the views as the occasion demands; we will see their equivalence.

For the parton densities, the multiplicative view will result in the following formula:

$$f_{j/H}(\xi) = \sum_{j'} \int_{\xi^-}^{1+} \frac{dz}{z} Z_{jj'}(z, g, \epsilon) f_{(0)j'/H}(\xi/z). \quad (8.11)$$

On the right-hand side is a bare parton density for a parton of flavor j' . Here a bare parton density is defined directly by whichever of operator formulae like (6.31) is appropriate, with the convention that the field operators are bare fields (i.e., that have canonical (anti)commutation relations). The theorem of renormalization is that one can obtain UV-finite parton densities $f_{j/H}(\xi)$ by a proper choice of the renormalization factor $Z_{jj'}$ in (8.11). The multiplication is in the sense of a convolution in the longitudinal momentum fraction and of matrix multiplication on the flavor indices. In the $\overline{\text{MS}}$ scheme, the renormalization factor is a function only of the ratio of the momentum fractions, the renormalized coupling and the dimension of space-time.

We have written limits ξ^- and $1+$ in the integral over z in (8.11), with the same meaning as in factorization formulae, such as (8.7). The upper limit is set by the renormalization

kernel (which includes a delta function at $z = 1$). The lower limit is set by the bare parton density, which is non-zero only for $\xi/z \leq 1$.

8.3.3 Polarization dependence

Formula (8.11) applies both to the unpolarized densities and to the various kinds of polarized densities (helicity, transversity, etc.). The transformations of the densities under rotations and parity imply that there is no mixing between the different kinds of polarized density. That is, one copy of (8.11) applies to the unpolarized densities, a second copy, with different renormalization factors, applies to the helicity densities, and a third copy, with yet different renormalization factors, applies to the transversity densities.

8.3.4 Regions giving UV divergences

An ordinary UV divergence (such as is canceled by renormalization of the Lagrangian) comes from regions where all the components of momenta in a subgraph get large. It might appear that the divergences in parton densities are different because they involve large values only for the minus and transverse components of loop momentum, as we saw in a calculational example. The momentum components are power-counted as $(k^+, k^-, k_T) \sim (P^+, \Lambda^2/P^+, \Lambda)$ where $\Lambda \rightarrow \infty$. However, this appearance that the divergence is of a new kind is misleading. We see this in light-front perturbation theory. Plus momenta are restricted to fractions of the external momenta, and even ordinary UV divergences also arise from large minus and transverse momenta, again with the power-counting $(P^+, \Lambda^2/P^+, \Lambda)$. An example is given by the self-energy graph that we calculated at (7.13).

The apparent difference arises because of a different choice of contour deformation: a Wick rotation of energy integrals in the usual case, and a contour integral in k^- for the light-front case. Of course, in a parton density with its integral over k^- , the light-front view is natural.

So the large k_T divergences in parton densities are actually genuine UV divergences to which we can apply normal methods of renormalization.

Further analysis proceeds by examining the momentum regions that give the UV divergence. We use the formalism in which the operators defining the parton density are time-ordered and the graphs are uncut. We take it for granted that renormalization has been applied in the Lagrangian, so that all UV divergences in self-energies and vertex corrections, etc., are canceled by counterterms. The remaining divergences involve loop momentum integrals that include the vertices that define the parton densities. Thus we represent the regions giving divergences by diagrams such as Fig. 8.5(a). In the upper part, labeled “UV”, the minus and transverse components of all momenta get large, with plus momenta obeying their normal restrictions (in particular not to be bigger than P^+). In the lower part, labeled “collinear”, the momenta stay finite. The collinear part includes the connecting lines of momentum l , while the UV part includes the lines of momentum k that go to the parton density vertices. In addition to being far off-shell, the momenta in the UV part have large negative rapidity relative to the target.

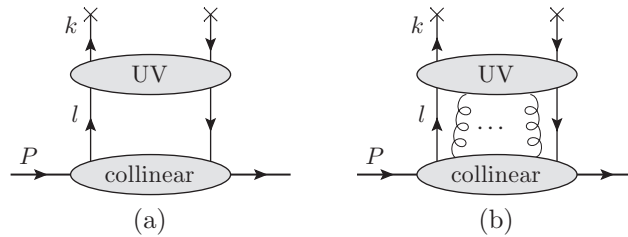


Fig. 8.5. (a) Regions giving UV divergence for pdf in renormalizable non-gauge theory or in a gauge theory (in light-cone gauge, $A^+ = 0$). The lines joining the UV and collinear subgraphs can be of any type, e.g., flavor of quark, antiquark or (transverse) gluon. (b) In a gauge theory arbitrary gluon connections between the collinear and UV subgraphs also give divergences.

We now do power-counting to determine the strength of the divergence and to determine what external lines are allowed for the UV part. For this we use the appropriate generalization of the rules for ordinary UV divergences given that we treat the components of UV momenta as having sizes $(P^+, \Lambda^2/P^+, \Lambda)$. By observing that such a momentum configuration can be obtained by a boost from a frame in which all the components of UV momenta are of order Λ , we readily see that the power-counting works just like the power-counting for hard scattering in DIS: Ch. 5. In the rest frame of a UV momentum, the collinear lines are indeed collinear to the fast-moving target. The basic degree of divergence for a graph with two lines connecting the UV and collinear subgraphs is logarithmic. We saw this in an example, and the property extends to higher-order graphs for the UV subgraph. The reason is that this subgraph is dimensionless, and so the power-counting of a UV divergence follows dimensional analysis in a renormalizable theory.

The estimate of the power can equally well be done in a fixed frame. In that case the key point in relating dimensional analysis to the size of the divergence of the integral is that in Lorentz-invariant quantities, a minus momentum k^- , which has two powers of Λ , always appears multiplied by a plus momentum k^+ , which has zero powers of Λ ; thus the power of Λ is the dimension of k^+k^- .

Therefore adding external collinear lines to the UV subgraph generally reduces its degree of divergence, and therefore gives convergence. The one exception, just as in our discussion of hard scattering in Ch. 5, is in a gauge theory when there are gluon lines with a minus index in the UV subgraph and a plus index at the attached gluon line. Thus in addition to regions of the form Fig. 8.5(a), we also have divergences with extra gluons joining the UV and collinear subgraphs, Fig. 8.5(b).

For this chapter we restrict our attention to a non-gauge theory, for which the catalog of divergent regions is Fig. 8.5(a). (This set of leading regions also applies to a gauge theory in $A^+ = 0$ gauge. But this chapter's treatment of renormalization does not genuinely apply, because of problems with divergences associated with the $1/k^+$ singularities in the gluon propagator.)

The details of constructing a renormalized parton density follow very closely the construction of matrix elements of renormalized local operators in conventional renormalization theory (e.g., Collins, 1984).

8.3.5 Momentum dependence of counterterms

There is one new feature, which concerns the dependence of the counterterms on external momenta. In conventional operator renormalization, when there is a logarithmic divergence, the counterterm can be chosen to be independent of momentum and mass. One general method of proof is to differentiate graphs with respect to the external momenta and/or masses. This reduces the degree of divergence, and thus for a logarithmic divergence shows that after differentiation there is no overall divergence, and therefore no counterterm is needed. There can be subdivergences in multiloop graphs, but these are canceled by their own counterterms; the overall divergence is what determines the need for a counterterm for a whole graph. In general, the counterterms are polynomials in momentum and mass with the degree of the polynomial equal to the degree of divergence.

We now apply the differentiation argument to the UV divergences in parton densities. The examples in Sec. 6.11 provide illustrations of the general principles. We will now show that differentiating with respect to a mass, or an external minus or transverse momentum, does reduce the degree of divergence. But differentiating with respect to an external plus momentum leaves the degree of divergence unchanged. Thus the divergence is allowed to be a function of plus momenta. This gives the convolution form in (8.11) for the renormalization of parton densities, rather than the multiplicative form that applies to local operators.

Differentiating a graph with respect to an external momentum gives a sum over terms where particular propagator (or numerator) factors are differentiated. So we consider a generic propagator, carrying an internal momentum k and an external momentum P :

$$\frac{1}{(P-k)^2 - M^2} = \frac{1}{2(P^+ - k^+)(P^- - k^-) - (\mathbf{P}_T - \mathbf{k}_T)^2 - M^2}. \quad (8.12)$$

The external momentum may be off-shell and may have non-zero transverse momentum. The UV divergence concerns the situation where \mathbf{k}_T and k^- go to infinity with k^+ fixed. There are three cases:

1. Differentiation of (8.12) with respect to P^+ reduces the dimension by one, but introduces a factor of a minus momentum:

$$\frac{d}{dP^+} \frac{1}{(P-k)^2 - M^2} = \frac{-2(P^- - k^-)}{[2(P^+ - k^+)(P^- - k^-) - (\mathbf{P}_T - \mathbf{k}_T)^2 - M^2]^2}. \quad (8.13)$$

In power-counting for the degree of divergence, the factor k^- in the numerator is treated as k_T^2 rather than as the single power k_T that matches its dimension. Thus the degree of divergence is unaffected by differentiating with respect to P^+ .

This is a general result: in Lorentz-invariant quantities, a plus momentum always appears multiplied by a minus momentum. Thus the unchanged degree of divergences is effectively a consequence of invariance under boosts in the z direction.

2. Differentiation with respect to a mass M or transverse momentum \mathbf{P}_T brings no extra factor; this reduces the degree of divergence by one unit, just as with local operators.
3. Differentiation with respect to an external minus momentum P^- gives an extra reduction of the degree of divergence, by two units instead of one unit.

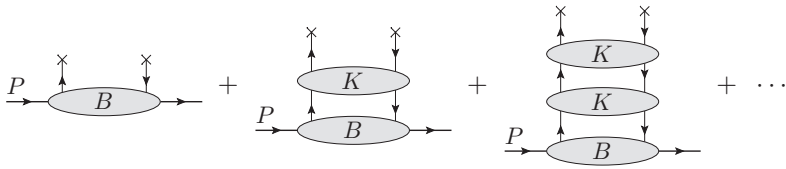


Fig. 8.6. Ladder decomposition of graphs for a bare parton density in terms of two-particle irreducible subgraphs.

When we use $\overline{\text{MS}}$ renormalization, the counterterms are just the divergent pole parts, so the coefficients of the poles obey the above rules for lack of dependence on minus momenta, transverse momenta and masses. In a general renormalization scheme, it is permitted to perform a further *finite* renormalization which does depend on these momentum components and masses. We choose not to.

We now summarize the form of the divergence in a parton density as

$$\int \frac{dl^+}{l^+} H(l^+, k^+) \int dl^- d^{2-2\epsilon} l_T L(l, P), \tag{8.14}$$

where H denotes the divergence of a UV subgraph. Since the divergence is independent of l^- and l_T , the integral over these variables can be confined to the collinear subgraph, corresponding to the rules for a parton density, in fact. But the UV and collinear parts are linked by an integral over l^+ .

Now parton densities are invariant under boosts in the z direction. Generally we will arrange for the factors in formulae such as (8.14) to be boost invariant. Notice that this is the case for the measure dl^+ / l^+ of the convolution. Then the UV divergence factor H must be a function, not of k^+ and l^+ separately, but only of their ratio. This gives the kinematic dependence of the renormalization factor Z_{jj} : it is a function of the ratio between the fractional momentum ξ of the renormalized parton density and the fractional momentum of the bare parton density.

8.3.6 Ladder graphs and renormalization

In this section, we will prove the renormalization theorem for parton densities, and we will see how the subtractive counterterm formalism is set up. The methodology (Collins, 1998a) is inspired by Curci, Furmanski, and Petronzio (1980).

The issue that makes the discussion quite non-trivial is that the characterization of UV divergences just given is somewhat incomplete. It assumed that we could assign the estimate $(P^+, \Lambda^2/P^+, \Lambda)$ uniformly to all the different momenta in the UV subgraph. But in fact there can be a variety of sizes.

Notation

A given graph for a bare parton density can have many decompositions of the form of Fig. 8.5(a). Given that they all have the two subgraphs connected by two lines, a convenient way to enumerate all possibilities is to perform a ladder decomposition, as in Fig. 8.6.



Fig. 8.7. Examples of topologies of graphs for the ladder rung K in Fig. 8.6. The lines and vertices are of any type allowed by the theory. The shortness of the lines at the lower end indicates that these propagators are amputated.

Each of the objects B and K is a sum over two-particle irreducible (2PI) graphs multiplied by full propagators for the upper two lines. Typical examples of graphs for K are shown in Fig. 8.7. They are connected and have two upper external lines and two lower external lines. Propagators with all possible corrections are used for the upper lines, but the lower lines are amputated. The two-particle irreducibility of the core part of K means that its top cannot be disconnected from the bottom by cutting only two lines; at least three lines must be cut. The base of the ladder, B , similarly has two propagators on its upper side times a 2PI amplitude, but it is now connected to the target state, including a bound state wave function if needed. The types of the lines can be any that is allowed in the theory.

We therefore represent the bare parton density for a parton of type j as a sum over ladder graphs with different numbers of rungs:

$$\begin{aligned}
 f_{(0)j} &= Z_j V(j) \sum_{n=0}^{\infty} K^n B \\
 &= Z_j V(j) \frac{1}{1 - K} B.
 \end{aligned}
 \tag{8.15}$$

The products are in the sense of a convolution, i.e., an integral over the momentum of the loop joining the factors, and sums over the flavor, color and spin indices, just as in (8.2).

At the top of the ladder we have the vertex defining the parton density, and in (8.15) we denote it by the factor V . A complete notation is cumbersome:

$$V(\xi P^+, j, s; k, j_1, c, c', \alpha, \alpha') = \delta(\xi P^+ - k^+) s_{\alpha\alpha'} \delta_{jj_1} \delta_{cc'},
 \tag{8.16}$$

which is set up to be used in the convolution notation, as in (8.2). The color and spin indices on the two attached parton lines are (c, α) and (c', α') . There is a common flavor index j_1 for the two lines. We let $s_{\alpha\alpha'}$ be the matrix with which the vertex couples the spin indices, e.g., $\gamma^+ / 2$ for an unpolarized quark density.

We require that both of K and B are Green functions of renormalized fields, so that they are UV finite. Since we define the bare parton density by an expectation value of bare operators, we inserted in (8.15) a factor of the wave function renormalization Z_j for the field for parton j .

The rung factor is

$$K(k_1, j_1, c_1, c'_1, \alpha_1, \alpha'_1; k_2, j_2, c_2, c'_2, \alpha_2, \alpha'_2).
 \tag{8.17}$$

Here, k_1 is the momentum of each of the upper lines, and j_1 is the flavor, while (c_1, α_1) and (c'_1, α'_1) are color and spin indices for the upper lines. The other variables are for the lower lines. There is also dependence on the coupling etc which is not indicated. Similarly for the

base of the ladder we write

$$B(k, j_1, c_1, c'_1, \alpha_1, \alpha'_1; P, S). \tag{8.18}$$

Note that if the target is an elementary particle, as in our calculational examples in Sec. 6.11, then the base factor B will be just a delta function, e.g.,

$$B(k, j_1, c, c', \alpha, \alpha'; P, S) = (2\pi)^{4-2\epsilon} \delta^{(4-2\epsilon)}(l - P) \delta_{j_1, \text{target}} \times \text{spin density matrix.} \quad (\text{Elementary target}) \tag{8.19}$$

Just as in (8.4), the two lines joining neighboring rungs (V , K , or B) have equal flavors. But we have allowed unequal values for the spin and color indices. But then we observe that V times any number of K s is color singlet, and so gives a coefficient times a unit matrix in color space. Hence we only use K and B in combinations with a diagonal sum over colors at their upper end, and so we write, for example,

$$\sum_{c_1} K(k_1, j_1, c_1, c_1, \alpha_1, \alpha'_1; k_2, j_2, c_2, c'_2, \alpha_2, \alpha'_2) = K(k_1, j_1, \alpha_1, \alpha'_1; k_2, j_2, \alpha_2, \alpha'_2) \delta_{c_2, c'_2}. \tag{8.20}$$

In the mathematical manipulations that follow, K is to be thought of as a matrix, with two composite indices, V as a row vector, and B as a column vector.

Divergences, subtractions, renormalization

We now define a renormalized parton density by the standard procedure of subtracting counterterms for each subgraph with an overall UV divergence. We first remove the wavefunction renormalization factor Z_j . Then we consider the UV divergences in one term VK^nB . Each possible divergent subgraph in Fig. 8.5(a) is associated with a subgraph consisting of V and some number $N_1 > 0$ of the nearest rungs.

A zero-rung graph VB therefore has no UV divergences. A one-rung graph VKB has one divergence, in the VK subgraph. We can cancel the divergence in VK by subtracting, for example, its pole part at $\epsilon = 0$, $VK \overleftarrow{\mathcal{P}}$, to give a finite result $VK(1 - \overleftarrow{\mathcal{P}})B$. The left arrow in $\overleftarrow{\mathcal{P}}$ signifies that the pole part is taken of everything to its left. The significance of the pole part is that it is independent of the external l^- and l_T of VK , since this is a property of the elementary UV divergence derived above. Thus $VK \overleftarrow{\mathcal{P}}$ is of the form of a vertex for a parton density at momentum fraction l^+/P^+ times a function of ξP^+ and l^+ . This will enable us to obtain multiplicative renormalization after we sum over all graphs and UV-divergent subgraphs. Naturally, the pole part may be replaced by any other operation that achieves the same effect, of canceling the divergence with a counterterm that is a coefficient times a vertex for a parton density.

From now on we will define $\overleftarrow{\mathcal{P}}$ to denote whatever such definition we choose to use, and the choice defines the renormalization scheme for the parton density. The standard choice is the $\overline{\text{MS}}$ scheme, Sec. 3.2.6, with its extra factor S_ϵ for each loop in a counterterm; see (3.16) and (3.18).

For a two-rung ladder, $VKKB$, we first cancel the divergence in the VK subgraph, to get $VK(1 - \overleftarrow{\mathcal{P}})KB$. The remaining divergence is in the two-rung part, and to cancel it we

can subtract $V K(1 - \overleftarrow{\mathcal{P}})K \overleftarrow{\mathcal{P}} B$. Here the second pole part is the pole part of everything to its left, i.e., the pole part of $V K(1 - \overleftarrow{\mathcal{P}})K$. After these subtractions the UV-finite result is $V K(1 - \overleftarrow{\mathcal{P}})K(1 - \overleftarrow{\mathcal{P}})B$. It is straightforward to extend this result to bigger ladders: we simply insert a factor $1 - \overleftarrow{\mathcal{P}}$ to the right of every factor of K .

We now convert this into a form that we use to demonstrate multiplicative renormalizability:

$$\begin{aligned}
 f_j &= V(j) \left[1 + K(1 - \overleftarrow{\mathcal{P}}) + K(1 - \overleftarrow{\mathcal{P}})K(1 - \overleftarrow{\mathcal{P}}) + \dots \right] B \\
 &= V(j) \sum_{n=0}^{\infty} \left[K(1 - \overleftarrow{\mathcal{P}}) \right]^n B \\
 &= V(j) \sum_{n=0}^{\infty} K^n B - V(j) \sum_{n=1}^{\infty} \sum_{n_1=1}^n \left[K(1 - \overleftarrow{\mathcal{P}}) \right]^{n_1-1} K \overleftarrow{\mathcal{P}} K^{n-n_1} B \\
 &= V(j) \sum_{n=0}^{\infty} K^n B - V(j) \sum_{n_1=1}^{\infty} \left[K(1 - \overleftarrow{\mathcal{P}}) \right]^{n_1-1} K \overleftarrow{\mathcal{P}} \sum_{n_2=0}^{\infty} K^{n_2} B \\
 &= V(j) \frac{1}{1 - K} B - V(j) \sum_{n=0}^{\infty} \left[K(1 - \overleftarrow{\mathcal{P}}) \right]^n K \overleftarrow{\mathcal{P}} \frac{1}{1 - K} B. \tag{8.21}
 \end{aligned}$$

To get from the second to the third line, we expanded all the products and classified the result by where the rightmost $\overleftarrow{\mathcal{P}}$ is. There is one term with no $\overleftarrow{\mathcal{P}}$ factors at all. The last line is in fact of the form of a coefficient convoluted with the bare parton density, (8.11). To see this, we first observe that the term $V(j) \frac{1}{1 - K} B$ is of the desired form, giving a contribution

$$Z_j^{-1} \delta_{jj'} \delta(z - 1) \tag{8.22}$$

to $Z_{jj'}$. Now a renormalization pole part is a coefficient times a vertex for a parton density. So the last term in (8.21) is a pole part times the $\frac{1}{1 - K} B$ factor in the bare parton density. Thus we also get something of the form of the right-hand side of (8.11). In fact we can write the renormalization coefficient as

$$Z_{jj'} V(j') = \frac{1}{Z_{j'}} \left[\delta_{jj'} \delta(z - 1) - V(j) \sum_{n=0}^{\infty} \left[K(1 - \overleftarrow{\mathcal{P}}) \right]^n K \overleftarrow{\mathcal{P}}(j') \right], \tag{8.23}$$

where the (j') argument of the last $\overleftarrow{\mathcal{P}}$ indicates that we restrict to graphs whose rightmost line pair has flavor j' .

This completes the proof of the renormalization theorem for parton densities, at least when the theory has no gauge fields. The proof also applies in a gauge theory (e.g., QCD) in $A^+ = 0$ gauge, if we assume that the non-trivial complications in this gauge do not matter.

For performing calculations, it is useful that the proof also applies to off-shell Green functions of the parton vertex operator, with the actual on-shell parton densities being obtained by applying LSZ reduction.

Nature of subtractive approach

The starting point of (8.21) was a modification of the definition of a parton density where all UV divergences were subtracted out. Then this was converted to a form that exhibited multiplicative renormalization of bare parton densities.

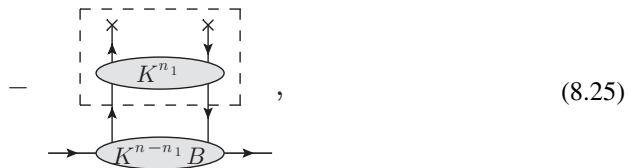
Now methods using subtractions are fundamental to all aspects of perturbative QCD, as we will see. So in the next few paragraphs I give further insights into the subtractive approach, with renormalization of parton densities giving an example of a general methodology.

Let us focus attention on the third line in (8.21). It starts with a sum over all graphs for the parton density partitioned by the number n of rungs; a generic term is $V K^n B$. Note that K and B themselves are sums of graphs of the appropriate irreducibility properties. Possible ways of getting UV divergences are enumerated by partitioning the product of rungs into two factors:

$$[V K^{n_1}] [K^{n-n_1} B], \tag{8.24}$$

where n_1 can range from 1 to n . Applying this to a single graphical structure, we have n ways of doing the partition. For each partition, there is a divergence where the momenta in the left part of (8.24) get large while the momenta in the right-hand part stay finite. The left factor corresponds to the upper part of Fig. 8.5(a).

An initial idea for removing the divergence is simply to subtract the UV pole part of the subdiagram $V K^{n_1}$. We can notate the subtraction diagrammatically as



where the box denotes the taking of the pole part, as in \overline{MS} renormalization.¹ Such subtractions do not actually remove the divergences correctly, for two related reasons. The first is the possibility of subdivergences: if $n_1 > 1$, the K^{n_1-1} factor has a pole from subdivergences, where only some of the rungs inside the box are in a UV region. The second is that of double counting: there can be further UV divergences when not only the momenta inside the box are UV, but also some momenta further down are also UV, which situation occurs if $n_1 < n$.

Both problems are solved by applying the pole-part operation only after subtractions have been made for subdivergences. In the third line of (8.21), this is done by the $(1 - \overline{\mathcal{P}})$ factors inside the $V K^{n_1}$ part.

To see this as a prevention of double counting, we imagine constructing the counterterms one by one, starting with the smallest, $n_1 = 1$. Let $C_{n_1}(V K^n B)$ be the counterterm for the n_1 -rung graph. It is made by applying minus the pole part to the original graph together

¹ Or the corresponding operation in some other renormalization scheme.

with the counterterms for smaller numbers of rungs:

$$C_{n_1}(VK^n B) = - \left[VK^{n_1} + \sum_{n'_1=1}^{n_1-1} C_{n'_1}(VK^{n_1}) \right] \overleftarrow{\mathcal{P}} K^{n-n_1} B. \tag{8.26}$$

The internal counterterms $C_{n'_1}$ remove subdivergences. As for double counting, consider the sum over n_1 : $\sum_{n_1=1}^n C_{n_1}(VK^n B)$. For the overall UV divergence in a particular VK^{n_1} , there will be contributions both from the original graph and from the counterterms for subdivergences in the set of terms $VK^{n_1} + \sum_{n'_1=1}^{n_1-1} C_{n'_1}(VK^{n_1})$. The use of (8.26) to define C_{n_1} deals with this problem.

Equation (8.26) is an example of the Bogoliubov operation in renormalization theory, and it provides a recursive definition of the counterterm. The recursion starts at $n_1 = 1$ where there are no subdivergences:

$$C_1(VK^n B) = -VK \overleftarrow{\mathcal{P}} K^{n-1} B. \tag{8.27}$$

It is not too hard to prove by induction that

$$C_{n_1}(VK^n B) = -[VK(1 - \overleftarrow{\mathcal{P}})]^{n_1-1} K \overleftarrow{\mathcal{P}} K^{n-n_1} B, \tag{8.28}$$

which gives the counterterms in the third line of (8.21).

An illustration of the box notation for counterterms is the case $n = 2$:

$$\begin{aligned}
 & \left(\text{Diagram 1} - \text{Diagram 2} \right) - \left(\text{Diagram 3} - \text{Diagram 4} \right) \tag{8.29} \\
 &= VK^2 B - VK \overleftarrow{\mathcal{P}} KB - (VK^2 - VK \overleftarrow{\mathcal{P}} K) \overleftarrow{\mathcal{P}} B \\
 &= VK(1 - \overleftarrow{\mathcal{P}}) K(1 - \overleftarrow{\mathcal{P}}) B.
 \end{aligned}$$

8.4 Renormalization group, and DGLAP equation

Renormalized quantities depend on the renormalization scale μ . When we apply the factorization theorem we will enable the effective use of perturbative theory in the hard scattering by setting μ to be of order Q . Therefore to make predictions, we need to transform parton

densities between different values of μ , for which we need their renormalization-group (RG) equations.

These are obtained by applying $d/d \ln \mu$ to (8.11) and using the RG invariance of the unrenormalized parton density. The resulting equations are known as the Dokshitzer-Gribov-Lipatov-Altarelli-Parisi (DGLAP) equations² (Altarelli and Parisi, 1977; Gribov and Lipatov, 1972; Dokshitzer, 1977). They have the form

$$\frac{d}{d \ln \mu} f_{j/H}(\xi; \mu) = 2 \sum_{j'} \int \frac{dz}{z} P_{jj'}(z, g) f_{j'/H}(\xi/z; \mu), \quad (8.30)$$

where, with its standard normalization, the (finite at $\epsilon = 0$) DGLAP evolution kernel $P_{jj'}$ obeys

$$\frac{d}{d \ln \mu} Z_{jk}(z, g, \epsilon) = 2 \sum_{j'} \int \frac{dz'}{z'} P_{jj'}(z', g, \epsilon) Z_{j'k}(z/z', g, \epsilon), \quad (8.31)$$

i.e., essentially

$$P = \frac{1}{2} \frac{d}{d \ln \mu} \ln Z, \quad (8.32)$$

with algebra (multiplication in particular) for Z being interpreted in the sense of convolutions on z , and in the sense of matrices on the partonic indices. Recall that the RG derivative when applied to such counterterms is just the beta function for a coupling times a derivative with respect to the coupling, and then summed over couplings. In the model Yukawa theory, this is

$$\frac{1}{2} \frac{d}{d \ln \mu} Z_{jk} = \left(-\epsilon \frac{g^2}{16\pi^2} + S_\epsilon^{-1} \beta_{g^2} \right) \frac{\partial Z_{jk}}{\partial g^2 / (16\pi^2)} + \left(-\epsilon \frac{\lambda}{16\pi^2} + S_\epsilon^{-1} \beta_\lambda \right) \frac{\partial Z_{jk}}{\partial \lambda / (16\pi^2)}. \quad (8.33)$$

Here $\beta_{g^2} \stackrel{\text{def}}{=} \frac{1}{2} dg^2 / d \ln \mu$, etc., with the normalizations like those of Sec. 3.5.2. Each β is a function of $S_\epsilon \lambda$ and $S_\epsilon g^2$, but not of ϵ separately (in the $\overline{\text{MS}}$ scheme). In QCD there would only be the β_{g^2} term.

8.5 Moments and Mellin transform

The connection to the renormalization of local operators can be exhibited by taking an integral with a power of ξ . We define

$$\tilde{f}_{j/H}(J) = \int_0^{1+} d\xi \xi^{J-1} f_{j/H}(\xi), \quad (8.34)$$

$$\tilde{Z}_{jj'}(J) = \int_0^{1+} dz z^{J-1} Z_{jj'}(z), \quad (8.35)$$

² The original derivations were rather different to the strict RG one presented here.

and similarly for the unrenormalized parton densities and the DGLAP kernels. Then (8.11) gives a matrix-multiplication form for the moments:

$$\tilde{f}_{j/H}(J) = \sum_{j'} \tilde{Z}_{jj'}(J) \tilde{f}_{(0)j'/H}(J). \quad (8.36)$$

The DGLAP equation similarly becomes

$$\frac{d}{d \ln \mu} \tilde{f}_{j/H}(J; \mu) = \sum_{j'} 2\tilde{P}_{jj'}(J; g) \tilde{f}_{j'/H}(J; \mu). \quad (8.37)$$

If J is allowed to range over general (complex) values, then we have constructed the Mellin transform of the parton density and shown that renormalization looks particularly simple for the Mellin transform. The Mellin transformation can be inverted to recover the parton densities in ξ space. In numerical calculations, it can be an advantage of the Mellin-transformed formulation that equations like (8.37) involve matrix multiplication rather than convolutions.

If J is restricted to non-negative integer value, and the combinations of parton and antiparton densities are used that correspond to local operators, as in (6.109), then we have the formula for renormalization of the local operators used in the OPE for DIS.

8.6 Sum rules for parton densities and DGLAP kernels, including in QCD

In Secs. 6.9.5 and 6.9.6, we derived number and momentum sum rules in a theory where no renormalization of parton densities was needed. We now extend the treatment to a renormalizable theory. The derivation will also apply to QCD, but only after we show that the renormalization theorems also apply to QCD.

Before renormalization we have bare parton densities in the UV-regulated theory. For a bare quark density, we derived a number sum rule in (6.92); the derivation applies also in QCD, since the Wilson line now needed between the quark and antiquark fields becomes unity when the fields are at the same position. The derivation must be applied to the bare parton densities in order to get the correctly normalized Noether current. In contrast, for the derivation of the momentum sum rule in QCD, the Wilson line requires a slight change in the derivation. Because of the extra factor ξ in the integrand of the sum rule (6.93), a derivative is needed with respect to the position of one of the fields in the quark density definitions. The derivative applies to both the field and the Wilson line, and the result is to give a covariant derivative of the quark field, and so to give the correct quark term in the energy momentum tensor. The gluon term also comes out correctly. After that the derivation is as before.

Each of these derivations applies to a particular moment of parton densities and results in a target matrix element of a Noether current, whose value we know exactly and which is finite. We now need to show that the sum rules also apply to *renormalized* densities and to obtain corresponding constraints on the renormalization coefficients. We first take the

inverse transformation to (8.36):

$$\tilde{f}_{(0) i/H}(J) = \sum_j \tilde{Z}_{ij}^{-1}(J) \tilde{f}_{j/H}(J), \tag{8.38}$$

where Z^{-1} is the matrix inverse of Z . The number sum rule for a quark q is that $\tilde{f}_{(0) q/H}(1) - \tilde{f}_{(0) \bar{q}/H}(1)$ is the number of this type of quark in the target H . Since this is finite, the corresponding renormalization coefficients are also finite: $\tilde{Z}_{qj}^{-1}(1) - \tilde{Z}_{\bar{q}j}^{-1}(1)$. Let us use the $\overline{\text{MS}}$ scheme, in which case finiteness only happens if the counterterms are zero, leaving the lowest-order terms. Thus we get the following sum rules for the first moments of the renormalization coefficients:

$$\tilde{Z}_{qj}^{-1}(1) - \tilde{Z}_{\bar{q}j}^{-1}(1) = \delta_{qj} - \delta_{\bar{q}j}, \tag{8.39a}$$

$$\tilde{Z}_{qj}(1) - \tilde{Z}_{\bar{q}j}(1) = \delta_{qj} - \delta_{\bar{q}j}, \tag{8.39b}$$

where the second line follows using the definition of the inverse matrix $Z^{-1}Z = I$. From (8.39b) and the sum rule for the bare parton densities follows the corresponding sum rule for the renormalized densities. Hence (6.91) applies to both bare and renormalized densities, provided the $\overline{\text{MS}}$ scheme is used.

The same argument applies to the momentum sum rule. It also leads to a sum rule for the renormalization coefficients:

$$\sum_j \tilde{Z}_{jj'}^{-1}(2) = \sum_j \tilde{Z}_{jj'}(2) = 1, \tag{8.40}$$

where the sum is over all flavors of parton: quarks, antiquarks, and gluon.

Combining the sum rules for Z with the definition of the DGLAP kernels (8.31) gives sum rules for the kernels:

$$\tilde{P}_{qj}(1) - \tilde{P}_{\bar{q}j}(1) = 0, \tag{8.41}$$

$$\sum_j \tilde{P}_{jj'}(2) = 0. \tag{8.42}$$

These sum rules have important testable consequences for the evolution of parton densities; they also provide useful checks on calculations.

8.7 Renormalization calculations: model theory

In this section we show how to calculate the renormalization of parton densities in the model Yukawa theory used earlier, to illustrate the principles without any confusion by the complications that arise in QCD.

8.7.1 Renormalization of the theory

The Lagrangian of the theory with renormalization for the interactions was given in (6.103). We use dimensional regularization and the $\overline{\text{MS}}$ scheme. We will express all quantities in

terms of renormalized couplings g , etc. As usual, to keep the dimension of the coupling fixed, we write the bare couplings in terms of the renormalized couplings with the unit of mass as $g_0 = \mu^\epsilon g(1 + \text{counterterms})$, etc. We will use a counterterm approach, as in Sec. 3.2. Thus we write the Lagrangian as the sum of a free Lagrangian that gives the free propagators, a basic set of interactions, with renormalized couplings, and a counterterm Lagrangian.

Of the renormalization factors in the Lagrangian, the ones that we will need in our calculations are for the self-energy, for which completely standard calculations give

$$Z_2 - 1 = -\frac{g^2 S_\epsilon}{32\pi^2 \epsilon} + \dots, \quad Z_2 M_0 - M = \frac{g^2 S_\epsilon M}{16\pi^2 \epsilon} + \dots, \quad (8.43)$$

where the dots indicate terms of yet higher order.

8.7.2 Unintegrated density

First we examine unintegrated, i.e., transverse-momentum-dependent, parton densities. The bare densities in the UV-regulated theory are, e.g.,

$$f_{(0)q/H}(\xi, \mathbf{k}_T) = \int \frac{d^2 w^- d^2 \mathbf{w}_T}{(2\pi)^3} e^{-i\xi P^+ w^- + i\mathbf{k}_T \cdot \mathbf{w}_T} \langle P | \bar{\psi}_0(0, w^-, \mathbf{w}_T) \frac{\gamma^+}{2} \psi_0(0) | P \rangle. \quad (8.44)$$

These have an immediate probability interpretation.

Since there are no extra divergences beyond those renormalized in the Lagrangian, the renormalized unintegrated quark density is obtained simply by using renormalized fields:

$$f_{q/H}(\xi, \mathbf{k}_T; \mu) = Z_2^{-1} f_{(0)q/H}(\xi, \mathbf{k}_T). \quad (8.45)$$

To get its RG equation, we observe that the bare parton density is a matrix element of bare fields with physical states, and hence is RG invariant. Taking a total derivative of the renormalized density with respect to the renormalization scale μ gives the RG equation of the renormalized density:

$$\frac{d}{d \ln \mu} f_{q/H}(\xi, \mathbf{k}_T; \mu) = -2\gamma_2 f_{q/H}(\xi, \mathbf{k}_T; \mu). \quad (8.46)$$

Here γ_2 is the anomalous dimension associated with the fermion field:

$$\gamma_2 = \frac{1}{2} \frac{d \ln Z_2}{d \ln \mu} = -\frac{g^2 S_\epsilon}{32\pi^2} + \dots, \quad (8.47)$$

which has a finite limit at $\epsilon = 0$.

8.7.3 Integrated density

For renormalization of the integrated densities, we use a counterterm approach with subtractions applied in Green functions of renormalized fields. Therefore we first write

(8.11) as

$$f_{j/H}(\xi) = \sum_j \int \frac{dz}{z} [Z_{j'}(g, \epsilon) Z_{jj'}(z, g, \epsilon)] [Z_{j'}^{-1} f_{(0)j'/H}(\xi/z)]. \tag{8.48}$$

Here the factor $Z_{j'}^{-1} f_{(0)j'/H}$ is the parton density with *renormalized* rather than bare fields used in its definition. Thus it is calculated using the standard Feynman rules for the theory and for the parton density; counterterms from the Lagrangian are used as needed. In compensation for the $Z_{j'}^{-1}$ factor the $Z_{jj'}$ factor is combined with a factor of $Z_{j'}$.

The renormalization factor gives UV-finite parton densities independently of the target state H . For calculations of $Z_{jj'}$, it is therefore convenient to choose the state to correspond to any of the elementary fields of the theory (as opposed to a bound state). To obtain the perturbation expansion of $Z_{jj'}$ from Feynman graphs, we expand (8.48) in powers of the renormalized couplings, and identify the necessary counterterms. We use the following expansions:

$$f_{j/H}(\xi) = \sum_{n=0}^{\infty} \left(\frac{g^2}{16\pi^2} \right)^n f_{j/H}^{[n]}(\xi) + \dots, \tag{8.49a}$$

$$f_{(0)j/H}(\xi) = \sum_{n=0}^{\infty} \left(\frac{g^2}{16\pi^2} \right)^n f_{(0)j/H}^{[n]}(\xi) + \dots, \tag{8.49b}$$

$$Z_{jj'}(z, g, \epsilon) = \sum_{n=0}^{\infty} \left(\frac{g^2}{16\pi^2} \right)^n Z_{jj'}^{[n]}(z, g, \epsilon) + \dots \tag{8.49c}$$

To avoid complicated formulae, we have written only the terms with the Yukawa coupling g , and the *dots indicate terms involving the other couplings*. The lowest-order term in Z is unity in the sense of a matrix in parton type and of a convolution in z :

$$Z_{jj'}^{[0]}(z) = \delta_{jj'} \delta(z - 1). \tag{8.50}$$

When the target is elementary, the lowest-order renormalized and bare parton densities are simply

$$f_{j/j'}^{[0]}(\xi) = f_{(0)j/j'}^{[0]}(\xi) = \delta(\xi - 1) \delta_{jj'}. \tag{8.51}$$

Note the notational distinction between “[0]” in a superscript to denote “lowest order”, and “(0)” to denote “bare” (normally in a subscript). Note also a *shift of notation* from Sec. 6.11: there we did not treat renormalization, so the expansion parameter was actually the bare coupling; now the expansion parameter is strictly the finite renormalized coupling.

The key equation for calculations of the renormalization factor is the n -loop expansion of the renormalization equation (8.48):

$$f_{j/k}^{[n]}(\xi) = \sum_{n'=0}^n \sum_{j'} \int \frac{dz}{z} Z_{jj'}^{[n']}(z, g, \epsilon) f_{(0)j'/k}^{[n-n']}(\xi/z). \tag{8.52}$$

8.7.4 One-loop renormalization calculations in model theory

Quark in quark

The one-loop case of (8.52) for the density of a quark in a quark is

$$\begin{aligned}
 f_{q/q}^{[1]}(\xi) &= \sum_j \int \frac{dz}{z} \left[(Z_2 Z_{qj})^{[0]}(z, g, \epsilon) (Z_2^{-1} f_{(0)j/q})^{[1]}(\xi/z) \right. \\
 &\quad \left. + (Z_2 Z_{qj})^{[1]}(z, g, \epsilon) (Z_2^{-1} f_{(0)j/q})^{[0]}(\xi/z) \right] \\
 &= (Z_2^{-1} f_{(0)q/q})^{[1]}(\xi) + (Z_2 Z_{qq})^{[1]}(\xi, g, \epsilon).
 \end{aligned}
 \tag{8.53}$$

We carried out the calculations of the bare version of $f^{[1]}$ in Sec. 6.11, and we now read off the necessary modifications to renormalize the parton densities.

Virtual correction to quark in quark

The one-loop virtual correction to the parton density Fig. 6.10(a) is to be modified by adding wave function and mass renormalization counterterms to the self-energy, so that we replace (6.114) by

$$\begin{aligned}
 \frac{g^2}{16\pi^2} f_{q/q}^{[1,V]}(\xi) &= -\delta(\xi - 1) \frac{g^2}{16\pi^2} \\
 &\times \int_0^1 dx \left\{ x \ln \left[\frac{\mu^2}{m^2 x + M^2(1-x)^2} \right] + \frac{2M^2 x(1-x^2)}{m^2 x + M^2(1-x)^2} \right\},
 \end{aligned}
 \tag{8.54}$$

in the limit that the UV regulator is removed, $\epsilon = 0$. Since this is finite by itself, no delta function contribution to $Z_2 Z_{qq}$ is needed: the UV divergence in the self-energy is removed by a counterterm from the interaction, and so does not affect renormalization of the parton density.

Real correction to quark in quark

For the real emission term, we need

$$\frac{g^2}{16\pi^2} (Z_2 Z)_{qq}^{[1]}(z, g, \epsilon) = -\frac{g^2 S_\epsilon}{16\pi^2 \epsilon} (1-z)
 \tag{8.55}$$

to cancel the UV divergence in (6.117), with the result that the real-emission contribution for the renormalized density $\epsilon = 0$ is

$$\frac{g^2}{16\pi^2} f_{q/q}^{[1,R]}(\xi) = \frac{g^2}{16\pi^2} \left\{ (1-\xi) \ln \left[\frac{\mu^2}{\xi m^2 + (1-\xi)^2 M^2} \right] + \frac{\xi(1-\xi)(4M^2 - m^2)}{\xi m^2 + (1-\xi)^2 M^2} \right\}.
 \tag{8.56}$$

Renormalization of quark in quark

The renormalization coefficient times Z_2 is therefore

$$(Z_2 Z)_{qq}(z, g, \epsilon) = \delta(z - 1) - \frac{g^2 S_\epsilon}{16\pi^2 \epsilon} (1 - z) + \dots, \tag{8.57}$$

so that

$$Z_{qq}(z, g, \epsilon) = \delta(z - 1) + \frac{g^2 S_\epsilon}{16\pi^2 \epsilon} \left[\frac{1}{2} \delta(1 - z) - 1 + z \right] + \dots \tag{8.58}$$

It is easily verified at order g^2 that this obeys the sum rule $\int_0^{1+} dz Z_{qq}(z) = 1$, as is necessary so that the number sum rule is obeyed. From (8.31) and (8.33) then follows the one-loop qq term in the DGLAP kernel:

$$P_{qq}(z) = \frac{g^2}{16\pi^2} \left[-\frac{1}{2} \delta(1 - z) + 1 - z \right] + \dots \tag{8.59}$$

Scalar in quark

Similarly we can renormalize the first off-diagonal term, in the distribution of a scalar parton in a quark from (6.118). The renormalization coefficient and the DGLAP kernel are

$$Z_{\phi q}(z) = -\frac{g^2 S_\epsilon}{16\pi^2 \epsilon} z + \dots, \tag{8.60}$$

$$P_{\phi q}(z) = \frac{g^2}{16\pi^2} z + \dots, \tag{8.61}$$

with a corresponding renormalized value for $f_{\phi/q}$.

Verification of sum rules

It is readily checked that the quark number and momentum sum rules are obeyed at this order:

$$\int_0^{1+} dz [P_{qq}(z) - P_{\bar{q}q}(z)] = 0, \tag{8.62}$$

$$\int_0^{1+} dz z [P_{qq}(z) + P_{\phi q}(z) + P_{\bar{q}q}(z)] = 0. \tag{8.63}$$

Note that these sum rules are written in their complete form, including a term for evolution of a quark to an antiquark $P_{\bar{q}q}$. Of course this last term is zero at one-loop order; the lowest order in which the $q \rightarrow \bar{q}$ occurs is order g^4 , from the graphs of Fig. 8.8.

Support properties

The continuum terms in all the above calculations of $Z_{jj'}$ and $P_{jj'}$ should be considered to have an implicit theta function to restrict z to lie between zero and one: $\theta(0 \leq z \leq 1)$.

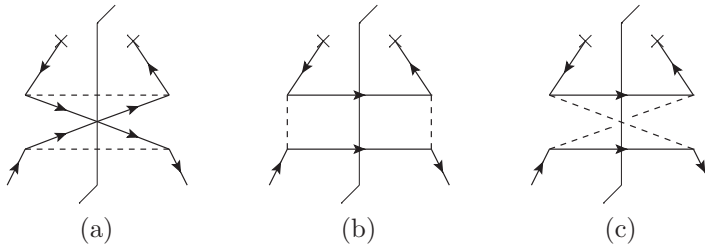


Fig. 8.8. Lowest-order graphs, order g^4 , for evolution of quark to antiquark.

8.8 Successive approximation method

I now outline an approach that creates a factorization formula like (8.5) as a series of successive approximations, with the parton model as the first term. This will motivate the technical proof, and will suggest a route for generalization in more complicated situations.

The parton model for the hadronic tensor $W^{\mu\nu}$ for electromagnetic DIS was derived from the handbag diagram as an approximation valid in the momentum region where the struck quark is collinear to the target. We call this the leading-order (LO) approximation to the $W^{\mu\nu}$, notated in Fig. 6.4(b). The graph and region continue to exist in the complete theory. Of course, the approximation breaks down when the transverse momentum or virtuality of the struck quark gets large, and there are graphs other than the handbag diagram. Let us regard the complete $W^{\mu\nu}$ as the LO approximation plus a remainder:

$$W^{\mu\nu} = W_{(LO)}^{\mu\nu} + (W^{\mu\nu} - W_{(LO)}^{\mu\nu}) \tag{8.64}$$

The hooks on the quark line of momentum k in the first term denote a parton-model approximator. This means that k^- and k_T are replaced by zero in the part of the diagram above the hook, and that projectors onto the leading power of the Dirac algebra are inserted. The result is a good approximation in the collinear region. We define the approximator to include an integral over all k , thereby obtaining a parton density, exactly as we defined it. Although not explicitly notated, we define the parton density to be renormalized, so that the LO approximation is finite. The unrestricted integral over k and the associated renormalization are the only changes from the parton approximator defined in Sec. 8.2.2.

We now analyze the remainder term, in parentheses. The most general leading-power contributions still have the form summarized in Fig. 8.2(a). However, if we take the hard-scattering subgraph to be lowest order, i.e., to be the top rung only, then in the parenthesized term in (8.64) this lowest-order case no longer gives a leading-power contribution, precisely because the subtraction cancels the relevant region.

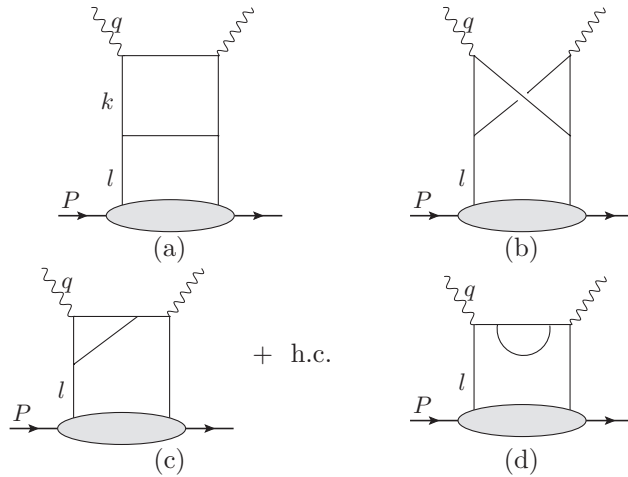


Fig. 8.9. Topologies of graphs needed for NLO approximation. The hermitian conjugate of graph (c) is also needed. UV counterterms are added to (c) and (d), as appropriate for the interaction and the current.

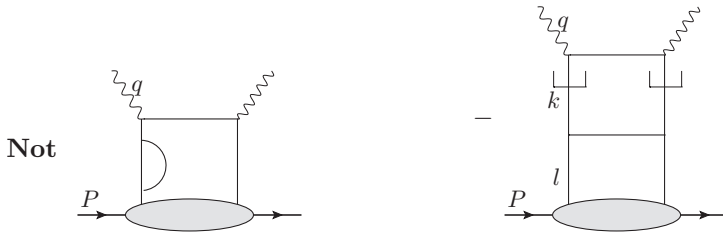


Fig. 8.10. Graphs like this with self-energy corrections are in in the handbag category, and are not used in Fig. 8.9.

Fig. 8.11. Subtraction graph.

For the leading approximation to the remainder term, we examine graphs of the form of Fig. 8.9. At the bottom, we have a complete parton-target amplitude, and at the top, we have a one-loop quantity. We are concerned with the case that the top loop is hard and the lower bubble is target-collinear. There is a sum over the flavors of the lines of the graphs. Notice that graph (a) is also among those included in the basic handbag diagram. Since the lower bubble represents an infinite sum over all graphs with the given external lines, it continues to represent the same quantity as in the handbag diagram. We do not include the case that there is a self-energy on the vertical parton lines, as in Fig. 8.10: these are included in the handbag category, for this part of the argument. To obtain the contribution to the parenthesized term in (8.64), we must subtract the parton-model approximation to graph (a), as symbolized in Fig. 8.11.

The graphs of Fig. 8.9 all have leading-power contributions when the momentum l of the line from the lower bubble to the upper one-loop subgraph, is collinear to the target. Contributions when l is larger will be dealt with in even higher-order corrections to the

hard scattering. The first graph (a) also has a leading-power contribution when the line k is target-collinear. But the subtraction, Fig. 8.11, cancels this contribution (to the leading power of k_T/Q). Thus the upper one-loop subgraph in all cases is dominated by large loop momenta.

We therefore apply a parton-model approximation on the line l , and obtain the following form for the NLO contribution to the structure tensor:

$$\begin{aligned}
 W_{(\text{NLO})}^{\mu\nu} = & \text{[Diagram 1]} + \text{etc.} + \\
 & + \text{[Diagram 2]} - \text{[Diagram 3]}
 \end{aligned}
 \tag{8.65}$$

The lower part again is a parton density, which we define to be renormalized. The definition of the approximator is that, in the upper part of the graph, l is replaced by just its plus component: $l \mapsto (l^+, 0, \mathbf{0}_T)$, with appropriate Dirac-algebra projectors. Thus the upper factor is essentially the one-loop approximation for DIS on an on-shell parton of longitudinal momentum l^+ . But there is a subtraction, to remove whatever was already taken care of at LO.

Further improvements can be made simply by iterating the procedure. In place of (8.64) we use

$$W^{\mu\nu} = W_{(\text{LO})}^{\mu\nu} + W_{(\text{NLO})}^{\mu\nu} + (W^{\mu\nu} - W_{(\text{LO})}^{\mu\nu} - W_{(\text{NLO})}^{\mu\nu}),
 \tag{8.66}$$

from which we obtain a further parton-model-like correction by analyzing the parenthesized term. This is the next-to-next-to-leading order (NNLO) approximation to DIS. Repeating the above procedure leads to a series of successive approximations that in fact correspond to an expansion in powers of $\alpha_s(Q)$.

8.9 Derivation of factorization by ladder method

We now make a complete derivation (Collins, 1998a) of factorization by using a decomposition in terms of 2PI subgraphs just as we did in Sec. 8.3.6 to discuss renormalization of parton densities.

8.9.1 Ladder expansion

The ladder decomposition is shown in Fig. 8.12, where B at the base of the ladders and K for the rungs are the same as in Fig. 8.6. There are two new features. The first is that

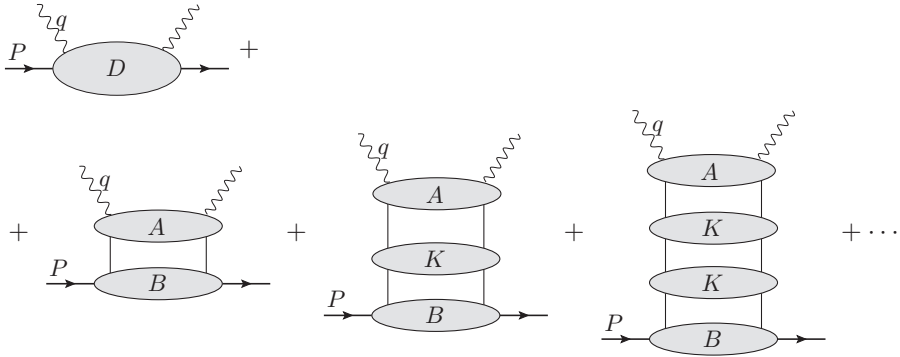


Fig. 8.12. Ladder decomposition of graphs for DIS. Each shaded bubble is 2PI in the vertical channel, except that K and B include the two full propagators on their upper side.

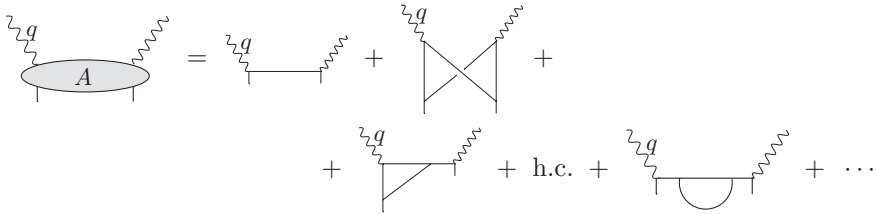


Fig. 8.13. Examples of topologies of graphs for the top A of ladder graphs for DIS in Fig. 8.12. The lines and vertices are of any type allowed by the theory. The shortness of the lines at the lower end indicates that these propagators are defined to be amputated.

because each current has two partonic lines we can have completely 2PI graphs. Their sum we denote by D , and these graphs are power-suppressed in Q because they have no decomposition of the generalized ladder form. The second new feature is that at the upper end of the ladder graphs we have, not a vertex for a parton density, but the sum A of 2PI graphs with two currents. Its expansion up to one-loop order is shown in Fig. 8.13.

Therefore we write a structure function (or the hadronic tensor $W^{\mu\nu}$) as

$$W = A \frac{1}{1 - K} B + D, \tag{8.67}$$

with exactly the same notation as in (8.15). The factor connected to the current has the functional dependence $A = A(q; k, j, c, c', \alpha, \alpha')$, where k is the momentum of the parton on the lower side of A , j is its flavor, and c, c', α and α' are indices for the color and spin of the parton, c and α on the left, and c' and α' on the right of the final-state cut.

8.9.2 Application of parton-model approximator

The proof of factorization generalizes to all orders the method of successive approximation of Sec. 8.8. Its implementation is by an algebraic method using the parton approximator

\overleftarrow{T} defined in (8.7) and (8.8), and the pole-part extractor $\overleftarrow{\mathcal{P}}$ used in Sec. 8.3 in the renormalization of parton densities.

To explain the algebraic method, I first apply it to low-order terms in the method of successive approximation, but applying it to the ladder sum (8.67). The first term is obtained by applying the parton approximator at the lower end of A :

$$W_{\text{ELO}} = A \overleftarrow{T} | V \frac{1}{1 - K(1 - \overleftarrow{\mathcal{P}})} B. \quad (8.68)$$

The parton approximator is applied to the complete top rung of the ladder, i.e., to A , rather than just to the lowest-order rung. So to label the resulting approximation, I use “ELO” for “extended leading order” rather than just “LO”. Unlike the use of the parton approximator in Sec. 8.2, there are no longer any restrictions on the internal momentum of any of the factors. But the parton densities are renormalized. This is accomplished by replacing the $1/(1 - K)$ factor by $1/(1 - K(1 - \overleftarrow{\mathcal{P}}))$ as already derived for the renormalization of parton densities. To use this definition, we require that the pole-part operation is only applied within the parton density, i.e., only between the $|$ symbol and the $\overleftarrow{\mathcal{P}}$ symbol. The reason for the emphasizing this is that the hard part $A \overleftarrow{T} |$ can have (finite) dependence on the UV regulator, which should not affect the pole-part operation; the pole-part operation is concerned only with defining the parton density, i.e., only with the objects to the right of the $|$ symbol.

The W_{ELO} term correctly treats the region where the parton below the A bubble is collinear. So in the remainder $W - W_{\text{ELO}}$, this region is suppressed. Therefore the region giving the first leading contribution to $W - W_{\text{ELO}}$ is where the hard subgraph consists of both A and one neighboring rung K . To obtain the associated contribution, we exhibit this first rung by writing the $1/(1 - K)$ factor as

$$\frac{1}{1 - K} = 1 + K \frac{1}{1 - K}. \quad (8.69)$$

Then the contribution in question is

$$\begin{aligned} W_{\text{ENLO}} &= \left[AK - A \overleftarrow{T} | V K(1 - \overleftarrow{\mathcal{P}}) \right] \overleftarrow{T} | V \frac{1}{1 - K(1 - \overleftarrow{\mathcal{P}})} B \\ &= \left[A(1 - \overleftarrow{T} | V)K + \text{c.t.} \right] \overleftarrow{T} | V \frac{1}{1 - K(1 - \overleftarrow{\mathcal{P}})} B. \end{aligned} \quad (8.70)$$

This is of the form of an ENLO coefficient convoluted with a complete renormalized parton density. The factor of $1 - \overleftarrow{T} | V$ between A and the first rung K suppresses the collinear region for the connecting momentum. A UV counterterm removes the UV divergence that is thereby introduced.

8.9.3 General case

The organization of the full proof is first to construct what we call the remainder, in which all leading behavior is subtracted out, and then to show that this remainder is the difference between the exact hadronic tensor W and a factorized form.

Remainder

The remainder is defined by the insertion of a $1 - \overleftarrow{T}|V$ factor between each rung in (8.67):

$$\begin{aligned}
 r &= \sum_{n=0}^{\infty} A (1 - \overleftarrow{T}|V) \left[K(1 - \overleftarrow{T}|V) \right]^n B + D \\
 &= A \frac{1}{1 - (1 - \overleftarrow{T}|V)K} (1 - \overleftarrow{T}|V) B + D \\
 &= A (1 - \overleftarrow{T}|V) \frac{1}{1 - K(1 - \overleftarrow{T}|V)} B + D. \tag{8.71}
 \end{aligned}$$

We now show that this is power suppressed. We also show that there are no extra UV divergences, unlike the case in (8.68) and (8.70), so that no UV subtractions need to be applied.

Before inserting $1 - \overleftarrow{T}|V$, we recall that leading-power contributions come from regions symbolized in Fig. 8.2(a). Thus inserting $\overleftarrow{T}|V$ between the hard and collinear subgraphs gives a good approximation in this region. Hence, inserting a factor $1 - \overleftarrow{T}|V$ gives a power suppression. In the general case, where we extend the loop-momentum integrations out of the core of the region, the factor $1 - \overleftarrow{T}|V$ gives a suppression which we can represent as

$$\left(\frac{\text{highest virtuality in collinear}}{\text{lowest virtuality in hard}} \right)^p. \tag{8.72}$$

Furthermore, in the rung A , closest to the virtual photon, we have virtualities of order Q^2 , while in the rung B , closest to the target, we have virtualities of order M^2 . Within a given rung, the leading-power contribution comes where all the lines have comparable virtualities, since leading-power contributions with regions of very different virtualities involve the structure of Fig. 8.2(a), with subgraphs connected by just two lines. Given that in (8.71) we have a factor $1 - \overleftarrow{T}|V$ between every 2PI rung, there is a suppression whenever there is a strong decrease of virtuality in going from one rung to its neighbor to the right. Thus we find the ladder part of (8.71) has an overall suppression of order

$$\left(\frac{M}{Q} \right)^p, \tag{8.73}$$

when it is compared to the structure function itself. The 2PI term D is power-suppressed by itself, and thus the whole of r is power-suppressed, as appropriate for what we wish to consider as a remainder.

This suppression of course gets degraded as one goes to higher order for the rungs, since the lines within K can have somewhat different virtualities. The larger a graph we have for K , the wider the range of virtualities we can have without meeting a significant suppression.

A potential problem arises because \overleftarrow{T} removes kinematic restrictions and thereby allows UV divergences to be induced, just as in the lowest-order approximation, (8.68). However, the UV divergences arise from the same kind of two-particle reducible structures as the leading regions, and the $1 - \overleftarrow{T}|V$ factors in r are just as effective at canceling the UV-divergence regions as they are at canceling leading-power contributions. Thus in fact r is finite and power suppressed. The UV divergences, with their attendant renormalization, only need to be treated when we expand the products.

Factorized form for $W - r$

I now show that $W - r$ factorizes. To present the algebra cleanly, I will first present the proof without renormalization of the parton densities, in the UV-regulated theory.

From (8.67) and (8.71), we find

$$\begin{aligned}
 W - r &= A \left[\frac{1}{1 - K} - \frac{1}{1 - (1 - \overleftarrow{T}|V)K} (1 - \overleftarrow{T}|V) \right] B \\
 &= A \frac{1}{1 - (1 - \overleftarrow{T}|V)K} \left[1 - (1 - \overleftarrow{T}|V)K - (1 - \overleftarrow{T}|V)(1 - K) \right] \frac{1}{1 - K} B \\
 &= A \frac{1}{1 - (1 - \overleftarrow{T}|V)K} \overleftarrow{T}|V \frac{1}{1 - K} B.
 \end{aligned}
 \tag{8.74}$$

This proof looks like straightforward linear algebra. In fact, there is a subtlety that \overleftarrow{T} is defined to set masses to zero on its left. The quotient $1/[1 - (1 - \overleftarrow{T}|V)K]$ is fundamentally defined as the infinite sum $\sum_{n=0}^{\infty} [(1 - \overleftarrow{T}|V)K]^n$, and the manipulations in (8.74) apply to this definition just as they do in ordinary linear algebra.

The last factor on the last line, $V[1/(1 - K)]B$ is exactly a bare parton density, so we see that $W - r$ is of the form of some coefficient convoluted with a parton density. This is a form of factorization, so we write

$$\begin{aligned}
 W &= \sum_j \int_{x^-}^{1^+} \frac{d\xi}{\xi} C_{B,j}(Q/\mu, \xi/x) f_{B,j}(\xi; \mu) \\
 &\quad + \text{terms with polarized parton densities} + \text{power-suppressed} \\
 &= C_B \otimes f_B + \text{polarized terms} + \text{p.s.c.}
 \end{aligned}
 \tag{8.75}$$

Here, ‘‘p.s.c.’’ denotes ‘‘power-suppressed correction’’, and we have defined a parton density by

$$f_{B,j}(\xi) = V \frac{1}{1 - K} B,
 \tag{8.76}$$

when the parton at V has flavor j and $k^+ = \xi P^+$. For simplicity, we only indicate explicitly the term with unpolarized densities; the polarized terms are similar in structure. The

coefficient function is

$$C_{B,j}(Q/\mu, \xi/x) = A \frac{1}{1 - (1 - \overleftarrow{T}|V)K} \overleftarrow{T}. \tag{8.77}$$

We use the “ \otimes ” notation to indicate a convolution in ξ and a sum over parton flavor, defined by the structure on the first line of (8.75).

We have one remaining complication, that of UV divergences. There are divergences in the parton density factor and in the coefficient function. Of course, these divergences cancel, since the left-hand side of (8.74) is finite, as we have already proved. As a first step, let us apply a UV regulator, e.g., dimensional regularization. We have defined all the rung factors as Green functions with renormalized fields. Thus the parton density $f_{B,j}(\xi)$ used in the above equations is a factor $1/Z_j$ times the bare parton density defined in terms of bare fields.

We now reorganize the (8.74) in terms of UV-finite quantities. From earlier work we know that the renormalized parton density is the convolution of a renormalization factor with the parton density f_B

$$f = G \otimes f_B. \tag{8.78}$$

So we simply define the renormalized coefficient function to be

$$C = C_B \otimes G^{-1}, \tag{8.79}$$

where the inverse in G^{-1} is in the sense of convolutions over ξ and matrix multiplication for parton flavor. Then, trivially $C_B \otimes f_B = C \otimes f$, and the factorization theorem becomes

$$\begin{aligned} W^{\mu\nu} &= C^{\mu\nu} \otimes f + \text{p.s.c.} \\ &= \sum_j \int_{x^-}^{1+} \frac{d\xi}{\xi} C_j^{\mu\nu}(Q/\mu, \xi, x) f_j(\xi; \mu) + \text{polarized terms} + \text{p.s.c.} \end{aligned} \tag{8.80}$$

8.10 Factorization formula for structure functions

In this section, we will convert the general structure of factorization, (8.80), into several forms directly suitable for practical calculations, to be carried out in Ch. 9. The formulae are also true in QCD, although their proof needs the enhancements to be given in Ch. 11. So the treatment will be presented with reference to its QCD applications.

8.10.1 Factorization for hadronic tensor

Polarization dependence appears in the trace over spin indices between the parton density and the hard-scattering factor. Exactly as in the parton model, Sec. 6.1, polarization can be allowed for by introducing a helicity density matrix $\rho_j(\xi)$ for the parton initiating the hard

scattering. Then factorization of the hadronic tensor has the form:

$$\begin{aligned}
 W^{\mu\nu} &= \sum_j \int_{x^-}^{1+} \frac{d\xi}{\xi} \text{Tr } C_j^{\mu\nu}(q, \xi P; \alpha_s, \mu) \rho_j(\xi; \mu) f_j(\xi; \mu) + \text{p.s.c.} \\
 &= C^{\mu\nu} \otimes \rho f + \text{p.s.c.}
 \end{aligned}
 \tag{8.81}$$

With a slight change of notation, the hard-scattering coefficient, $C_j^{\mu\nu}$, has acquired helicity indices, and is traced with the partonic helicity density matrix. It is to be thought of as giving DIS on a parton target of flavor j and fractional longitudinal momentum ξ . There is a sum over all parton flavors j and an integral over all kinematically accessible ξ . A convenient notation for the integral over ξ , the sum over j and the trace with ρ is the convolution symbol \otimes in the last line.

As explained in Sec. 6.5, the combination of $\rho_j f_j$ can be written in terms of the unpolarized densities f_j and asymmetry densities Δf_j and $\delta_T f_j$ for helicity and transversity, for the case of a spin- $\frac{1}{2}$ target. (A generalization is needed for higher spin targets like the deuteron.)

We express $C_j^{\mu\nu}$ in terms of scalar coefficient functions \hat{F}_{ij} by relations like those for the regular structure functions, (2.20), except for the use of the momentum of the struck (massless) parton instead of the momentum of the target hadron:

$$\begin{aligned}
 \text{Tr } C_j^{\mu\nu} \rho_j &= (-g^{\mu\nu} + q^\mu q^\nu / q^2) \hat{F}_{1j}(x/\xi, Q^2) \\
 &+ \frac{(\xi \hat{P}^\mu - q^\mu \xi \hat{P} \cdot q / q^2)(\xi \hat{P}^\nu - q^\nu \xi \hat{P} \cdot q / q^2)}{\xi \hat{P} \cdot q} \hat{F}_{2j}(x/\xi, Q^2) \\
 &+ i \epsilon^{\mu\nu\alpha\beta} \frac{q_\alpha S_{j,\beta}}{\hat{P} \cdot q} \hat{g}_{1j}(x, Q^2) + F_3 \text{ term} + \text{extra gluon term.}
 \end{aligned}
 \tag{8.82}$$

Here $\hat{P} = (P^+, 0, \mathbf{0}_T)$ is a massless projection of the target momentum, so that $\hat{k} \stackrel{\text{def}}{=} \xi \hat{P}$ is the momentum of the struck parton, in the approximation that is used in the hard scattering. An exact transcription of (2.20) would also include a \hat{g}_2 structure function associated with transverse quark spin. We omit it since \hat{g}_2 is zero to all orders of perturbation theory (Sec. 8.10.5). Therefore we need only the longitudinal polarization of the parton, and we assign it a spin vector $S_{j,\mu} = \lambda_j \hat{k}_\mu$, where λ_j is the parton's helicity. This is used with the \hat{g}_1 structure function.

In QCD, the gluon has spin 1, and when the hadronic target has spin greater than $\frac{1}{2}$, there is a possible term in the gluon's density matrix that flips helicity by two units: see Artru and Mekhfi (1990) and problem 7.11. This results in the "extra gluon term" in (8.82). I have left it as a (probably academic) exercise, to sort out the details (problem 8.3).

8.10.2 Factorization for structure functions

To get factorization formulae for the structure functions, we insert (8.82) in the factorization formula (8.81). Then we use the results from Sec. 6.5 that a parton in an unpolarized target is itself unpolarized and that its helicity is proportional to the target helicity. These results

were derived in a simple model theory, but they depend only on symmetry properties of the theory, and are therefore generally true. Hence

$$F_1 = \sum_j \int_{x^-}^{1+} \frac{d\xi}{\xi} \hat{F}_{1j}(Q/\mu, x/\xi; \alpha_s) f_j(\xi; \mu) + \text{p.s.c.}, \tag{8.83a}$$

$$F_2 = \sum_j \int_{x^-}^{1+} d\xi \hat{F}_{2j}(Q/\mu, x/\xi; \alpha_s) f_j(\xi; \mu) + \text{p.s.c.}, \tag{8.83b}$$

$$g_1 = \sum_j \int_{x^-}^{1+} \frac{d\xi}{\xi} \hat{g}_{1j}(Q/\mu, x/\xi; \alpha_s) \Delta f_j(\xi; \mu) + \text{p.s.c.} \tag{8.83c}$$

The second formula also applies to the longitudinal structure function $F_L \stackrel{\text{def}}{=} F_2 - 2xF_1$. Notice that:

- F_1 and F_2 only involve the unpolarized number densities;
- g_1 only involves the helicity asymmetry density;
- in the formula for F_2 the integration measure is $d\xi$ instead of $d\xi/\xi$;
- the coefficients are functions of x/ξ , rather than ξ and x separately;
- the transversity density $\delta_T f_j$ does not appear;
- the structure function g_2 does not have a formula. As we will see, its contribution to $W^{\mu\nu}$ is power suppressed, and therefore its leading-power approximation is zero.

The first two items depend on the parity invariance of the theory. In a parity non-invariant theory, it would be possible, for example, for partons to be polarized even when the parent hadron is unpolarized. We now give derivations of the other items.

8.10.3 Integration measure for F_2

The changed integration measure for F_2 is associated with its transformation under boosts of the target momentum. In the hadronic tensor (2.20), it multiplies the tensor $(P^\mu - q^\mu P \cdot q/q^2)(P^\nu - q^\nu P \cdot q/q^2)/P \cdot q$, which is linear in P . Now the coefficient function depends only on the momenta $\xi \hat{P}$ and q , but not on \hat{P} or ξ separately. Then in the part associated with the F_2 structure function, there appears the tensor $(\xi \hat{P}^\mu - q^\mu \xi \hat{P} \cdot q/q^2)(\xi \hat{P}^\nu - q^\nu \xi \hat{P} \cdot q/q^2)/\xi \hat{P} \cdot q$, which scales linearly with ξ . To obtain the correctly normalized structure function F_2 , we extract the factor ξ , which cancels the $1/\xi$ in the integration measure in (8.80). (There is further slight mismatch between the tensors, by a factor $1 + x^2 M^2/Q^2$, which is irrelevant to leading power in Q .)

8.10.4 Functional dependence of partonic structure functions

Both the hadronic tensor $W^{\mu\nu}$ and its hard-scattering counterpart $C_j^{\mu\nu}$ are dimensionless. Each of the partonic structure functions in (8.82) is also dimensionless, and the tensors

multiplying them are independent of Q^2 . Power-counting in a renormalizable theory therefore shows that order-by-order in perturbation theory all these quantities behave like Q^0 times logarithms of Q .

Each of the partonic structure functions in (8.82) is a Lorentz scalar, so the only kinematic variables it depends on are the invariants constructed out of its external momenta, i.e., Q^2 and $\xi \hat{P} \cdot q = \xi Q^2/(2x)$. The structure functions are also dimensionless. Therefore their independent arguments can be taken as Q/μ and x/ξ .

8.10.5 Transverse polarization

For the polarized structure functions, we first examine their scaling properties. In the Breit frame, the proton is highly boosted, so we count its momentum P as of order Q . When it has a longitudinal polarization λ , the spin vector S scales approximately as P , so that S is of order Q also. The tensor $i\epsilon^{\mu\nu\alpha\beta}q_\alpha S_\beta/P \cdot q$ associated with g_1 therefore scales as the zeroth power of Q , just like the tensors associated with F_1 and F_2 . But the tensor multiplying g_2 has the longitudinal part subtracted, in the $S_\beta - P_\beta S \cdot q/P \cdot q$ factor; it is suppressed in fact by order M^2/Q^2 for longitudinal polarization. Thus to leading power, for longitudinal polarization, we have a contribution to g_1 times its tensor, and this is proportional to the longitudinal polarization λ of the target. Correspondingly, the factorization formula (8.83c) for g_1 uses the helicity parton density Δf .

There remains the case of transverse spin, and associated with it the transversity distributions $\delta_T f$. First we observe that the transverse components of the spin vector are invariant under boosts in the z direction. For this case, the tensors multiplying both of g_1 and g_2 are of order M/Q .

Now the only way transverse-spin dependence enters into the factorization (8.80) is through the transversity density, and thus through a transverse polarization for quarks entering the hard scattering and the coefficient function. But we set masses to zero in the hard scattering, and as we now show, there is then exactly zero contribution from transverse quark polarization. (As shown in Sec. 7.5.5, rotation invariance prohibits a gluon distribution that is transverse-spin dependent.)

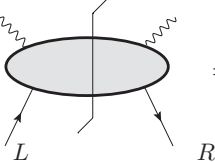
In the case of the lowest-order calculation, in Sec. 6.1.4, the reason for the zero contribution of transverse spin is quite elementary. In the parton-model hard scattering (6.19), spin dependence arises from the factor $\hat{k}(1 - \gamma_5 \lambda_j - \gamma_5 b_{jT}^i \gamma^i)$. The transverse-spin dependent term, with b_{jT} , gives a trace of an odd number of elementary Dirac matrices which is always zero. (Recall that $\gamma_5 = i\gamma^0 \gamma^1 \gamma^2 \gamma^3$ so that it counts as four elementary Dirac matrices.)

The same property generalizes to higher order. This is particularly clear in QCD. Let us go around the quark loop in which the struck quark is involved. There is an equal number of propagator numerators and vertices for gluons and photons. Except for the external line factor, each vertex and propagator numerator contains one Dirac matrix, giving a total number that is even. (This is where the masslessness of the calculation enters.) This is modified only on the external line factor with its extra odd number of Dirac matrices. Thus we get zero for the transverse spin dependence, as claimed.

The presence of subtractions in the hard scattering [see (8.77)] does not affect this argument. The subtractions involve kinematic approximants and the insertion of spinor projection matrices \mathcal{P}_A and \mathcal{P}_B . The spinor projections each have two elementary Dirac matrices, so that they leave unchanged the evenness or oddness of the number of Dirac matrices.

With couplings to a scalar field, as in a Yukawa theory, there is no Dirac matrix at the scalar vertex. Thus we can get an even number of Dirac matrices in the trace with a transversely polarized quark provided that we have an odd number of scalar vertices on the quark line. But for the leading power in Q , we must keep only those interactions with a dimensionless coupling. All such couplings (in a four-dimensional theory) involve an even number of scalar fields, as in a ϕ^4 coupling or an interaction between a scalar field and a gauge field. If there is an odd number of scalar vertices on the quark loop including the external line, then some other quark loop also has an odd number of scalar vertices. This other loop has no transverse polarization matrix, and therefore an odd number of Dirac matrices, and therefore its Dirac trace vanishes.

The result is that in all cases the coefficient function with the transversity distribution is zero at the leading power of Q . Now transverse-spin dependence of the hard scattering arises from off-diagonal terms in the helicity density matrix. So the result on g_2 can be expressed by saying that in the hard scattering there is helicity conservation, i.e., there is no interference between a left-handed quark and a right-handed quark:



$$= 0. \quad (8.84)$$

Note that helicity is defined in only at space-time dimension 4. But our derivation used only the evenness or oddness of the number of Dirac matrices along quark lines, so the derivation applies without an anomaly when we use dimensional regularization in calculations.

Discussion of g_2 and of transverse-spin dependence in fully inclusive DIS therefore requires us to go beyond the leading power of Q , in fact to twist-3 operator contributions in the jargon of the subject. This is beyond the subject matter of this book. Unlike the case for the unpolarized and helicity parton densities, DIS is not a good place to measure the transversity density.

The whole of the above discussion assumed the target had spin $\frac{1}{2}$, in which case the target's spin state is completely specified by the spin vector S^μ . More general cases, notably spin 1, as for a deuteron target, can be discussed. But the results are of mostly lesser interest.

8.11 Transverse-spin dependence at leading power?

An interesting line of research over the past two decades has found useful observables that depend on transverse spin at the leading power. In this section, we give a general

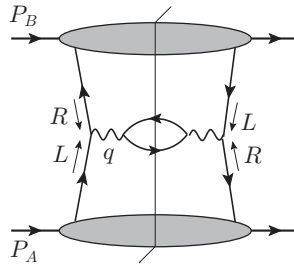


Fig. 8.14. At leading power, LO Drell-Yan has a double-transverse spin asymmetry from amplitudes such as this. Both hadrons are transversely polarized.

characterization of these observables. See, e.g., Boer (2008) for a detailed review, and see Sec. 13.16 for examples.

The whole discussion is conditioned by chirality conservation in the massless limit and hence in the hard scattering. Chirality conservation is the correct generalization of helicity conservation when we include antiquarks; it means the helicity of a quark and the negative of helicity for an antiquark. Thus the vertices of gauge bosons couple a left-handed quark to a left-handed quark or to a right-handed antiquark, but not to a right-handed quark or a left-handed antiquark.

There are two ways of getting dependence on transverse spin. One is to find a more general hard scattering that has off-diagonal helicity dependence. The other is to find parton-density-like objects with more general spin dependence than ordinary parton densities.

8.11.1 Hard scattering with transverse spin

Transverse spin gives one unit of helicity flip in a parton density, and this must be matched in the hard scattering to get a leading-power effect. To avoid violating chirality conservation, we need a hard scattering with (at least) another pair of external quark lines, so that we have two compensating helicity flips (Artru and Mekhfi, 1990). Such processes are needed to measure transversity densities.

One possibility is in hadron-hadron collisions, where the hard scattering is initiated by two partons, one out of each hadron (to be treated in detail in Ch. 14). A classic example is the Drell-Yan process, Sec. 5.3.7, where the lowest-order hard scattering is quark-antiquark annihilation to a virtual photon. If both initial-state hadrons are transversely polarized, then (Ralston and Soper, 1979) we can have a leading-power double-spin asymmetry, as shown in Fig. 8.14.

Another similar possibility is in semi-inclusive DIS, where the cross section is differential in a final-state hadron. In Ch. 12, we will generalize factorization to include a fragmentation function that parameterizes the conversion of an outgoing quark to a jet containing the detected hadron(s). Then the interference diagram Fig. 6.2, which gave zero in ordinary DIS, gets a fragmentation function inserted into it, Fig. 8.15. The fragmentation function needs to be off-diagonal in helicity for our purposes. It could be that the outgoing hadron

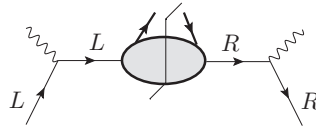


Fig. 8.15. Interference between left-handed and right-handed initial quark in DIS with the fragmentation providing the necessary helicity flip.

has its polarization measured; a practical example (Efremov, 1978; Artru and Mekhfi, 1990) is production of the Λ^0 , whose decay allows its polarization to be measured. In addition, since fragmentation is non-perturbative, the chiral symmetry breaking of full QCD allows the fragmentation function to break chirality conservation while keeping leading-power behavior (Collins, Heppelmann, and Ladinsky, 1994), provided a suitable final-state distribution is measured.

8.11.2 Transverse-momentum-dependent densities, etc.

Finally, some reactions require the use of transverse-momentum-dependent (TMD) parton densities (and/or fragmentation functions). As we will see in Ch. 13, a TMD number density can have a correlation between the azimuthal angle of a parton and transverse spin of the target. Thus at leading power, we can have dependence on the transverse spin of a target hadron without needing transverse-spin dependence in the hard scattering.

A considerable number of variations on this idea exist, especially when fragmentation functions are included (Boer, 2008).

Exercises

8.1 (****) In a renormalizable theory, it is natural to define the light-front creation and annihilation operators by Fourier transformation of the renormalized fields instead of bare fields, since it is the renormalized fields that have finite Green functions. For a field with wave function renormalization factor Z , the commutation relations of the creation and annihilation operators are enhanced by a factor $1/Z$, which is infinite unless the anomalous dimension of the field is zero at the UV fixed point. This messes up the normalizations of the basis states (7.23) by an infinite amount, in the limit that the UV cutoff is removed.

Find a good way of specifying basis states in the renormalized theory in the limit that the UV cutoff is removed. What is the relation between these states and the standard basis states in the cutoff theory? [Conjectures and suggestions: 1. Some of the techniques used in treating factorization later in this book may be useful. 2. Fourier-transforming at fixed x^+ corresponds to maximal uncertainty on k^- . It may help to perform a local average over x^+ . 3. Useful references include: Yamawaki (1998); Nakanishi and Yamawaki (1977); Heinzl (2003); Sec. 4 of Heinzl and Ilderton (2007); Nakanishi and Yabuki (1977); Steinhardt (1980).]

- 8.2** (***) Find the relation between parton densities and the basis found in problem 8.1.
- 8.3** (***) *Extension of problem 6.8 to full QCD:* Generalize the work in this chapter to deal with DIS on a polarized spin-1 target like the deuteron. What is the form of the extra gluonic term indicated in (8.82)? What is the corresponding NLO hard-scattering coefficient corresponding to this extra term? Notes:
- Much of the necessary work on defining structure functions has been done by Hoodbhoy, Jaffe, and Manohar (1989). But it is good to check their results. Note that they used the OPE rather than factorization for their QCD analysis. But they restricted their attention to the quark operators, and did not indicate what to do with gluon operators.
 - Since the gluon has spin 1, their analysis definitely needs generalization to deal with a gluon-induced hard scattering. You will need to work out a version of their analysis to the hard-scattering coefficient for a gluon $C_g^{\mu\nu}$. This will result in significant changes, since there are no gluons of helicity zero. Hoodbhoy, Jaffe, and Manohar (1989) also normalized the polarization vector E^μ of a spin-1 particle of mass M to $E^2 = -M^2$, which is clearly a bad idea for a massless particle.
 - You should find another polarized gluon density related to linear gluon polarization (so that its operator gives a helicity flip of 2 units); see Artru and Mekhfi (1990).
 - You should match the results of this problem with your solution of problem 7.11 and the results in Artru and Mekhfi (1990).
 - In the light of the above, you may find better characterizations of the structure functions on a spin-1 target.
 - I do not guarantee the phenomenological importance of the results of solving this problem.